

# ICHEP 2024

## PRAGUE

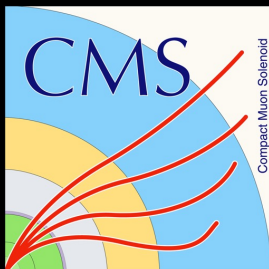


ichep2024

42<sup>nd</sup> International Conference on High Energy Physics

July 17-24 • 2024 • Prague • Czech Republic

## Performance of electrons and photons at CMS and recent developments



**Riccardo Salvatico**<sup>1</sup>  
on behalf of the CMS Collaboration

<sup>1</sup> CERN

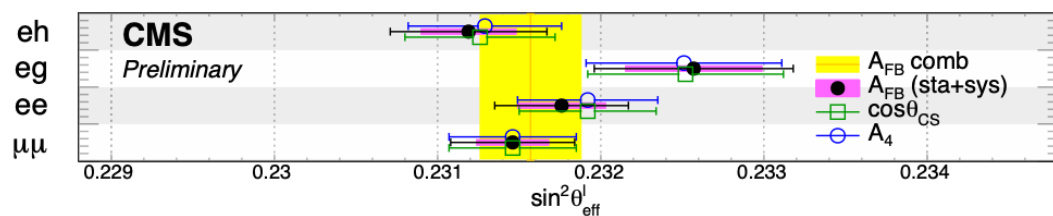




Critical for the success of the CMS physics program, both in terms of standard model measurements and searches

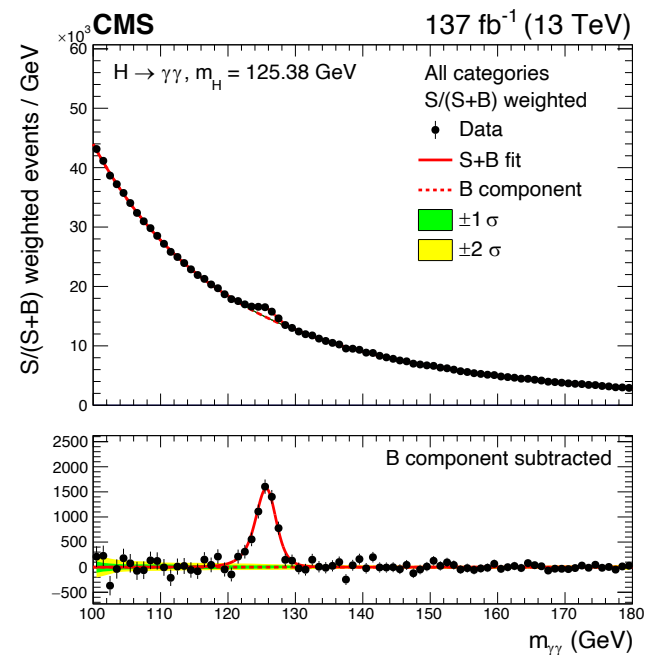
## Run2 $H \rightarrow \gamma\gamma$ production cross section and couplings

### Effective leptonic weak mixing angle



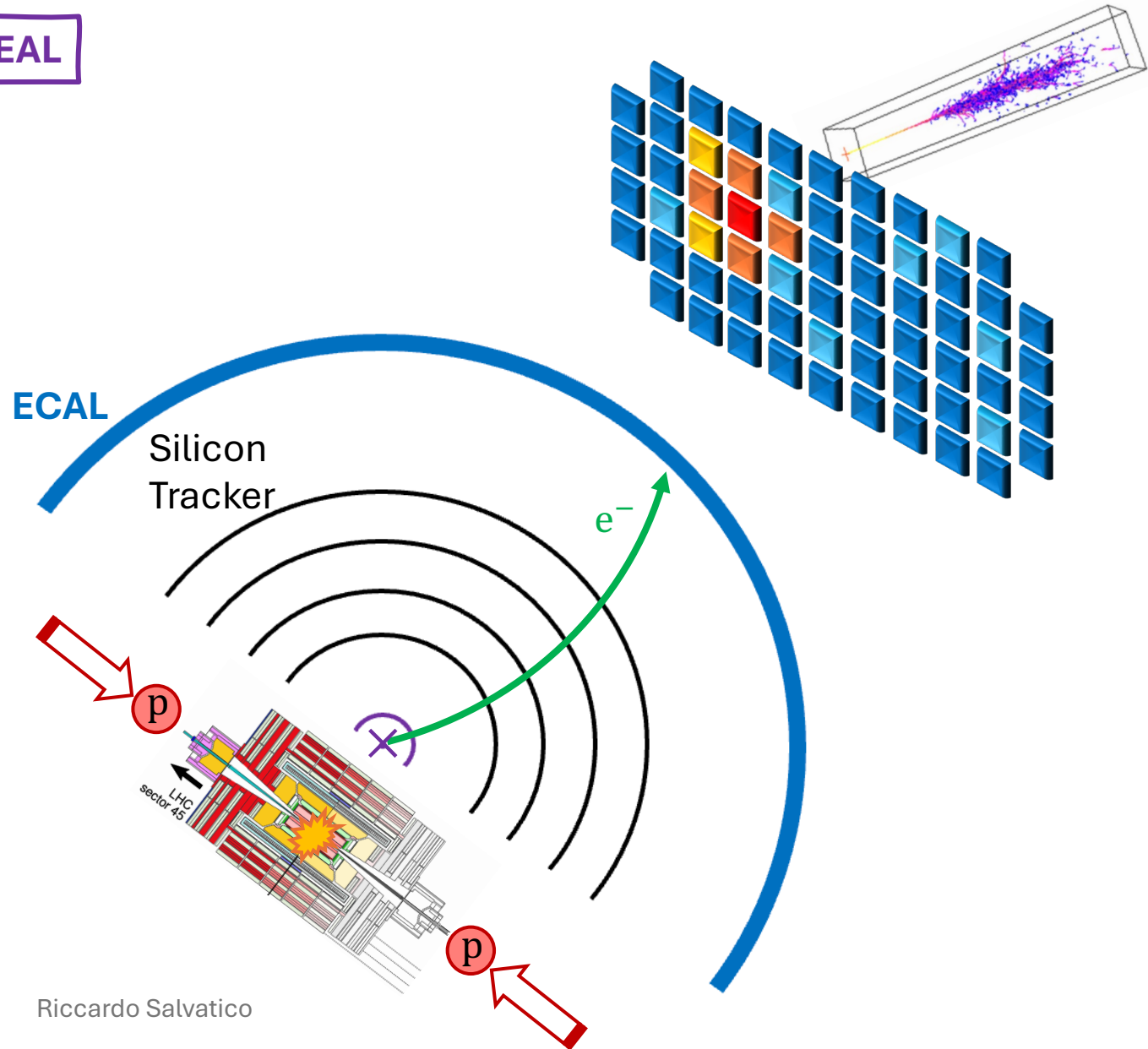
### At ICHEP 2024:

- $H \rightarrow \gamma\gamma$  and  $H \rightarrow 4\ell$  cross sections and couplings in Run3 (see [Jan Lukas' talk](#))
- H boson mass and width (see [Badder's talk](#))
- Several searches with photons in the final state (see [Rocco's talk](#) for SM, [Jyoti's talk](#) for BSM)
- Compressed SUSY with electrons in the final state (see [Margaret's talk](#))
- etc.



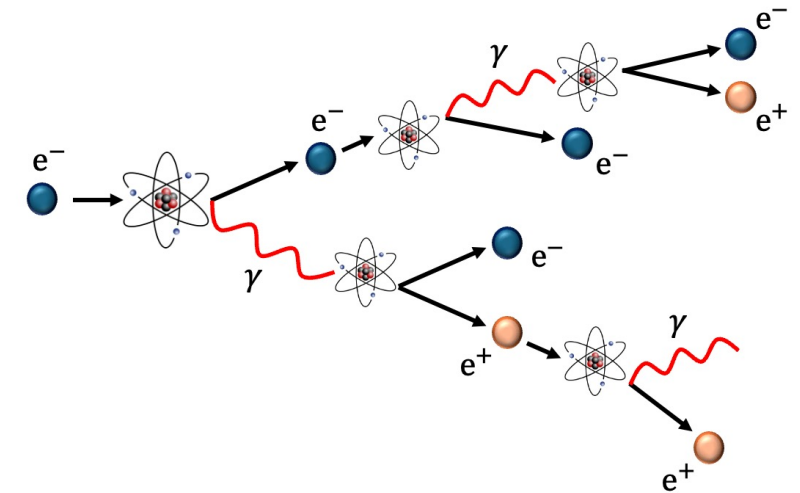


IDEAL



A hit in the ECAL

→ an EM shower in a small **cluster** of  $PbWO_4$  crystals

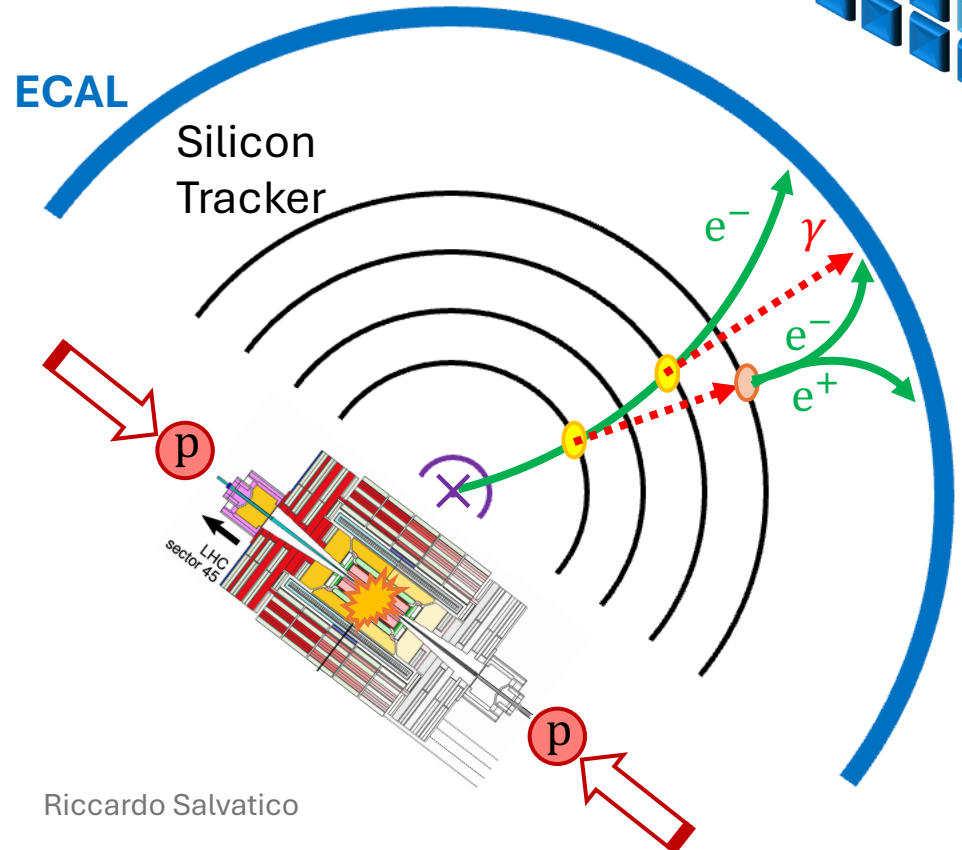
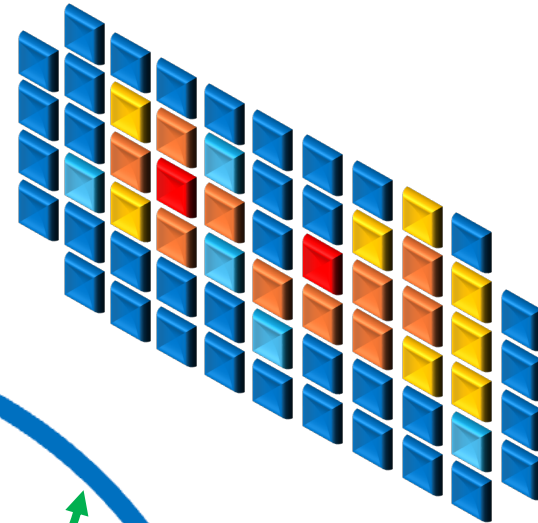




REAL

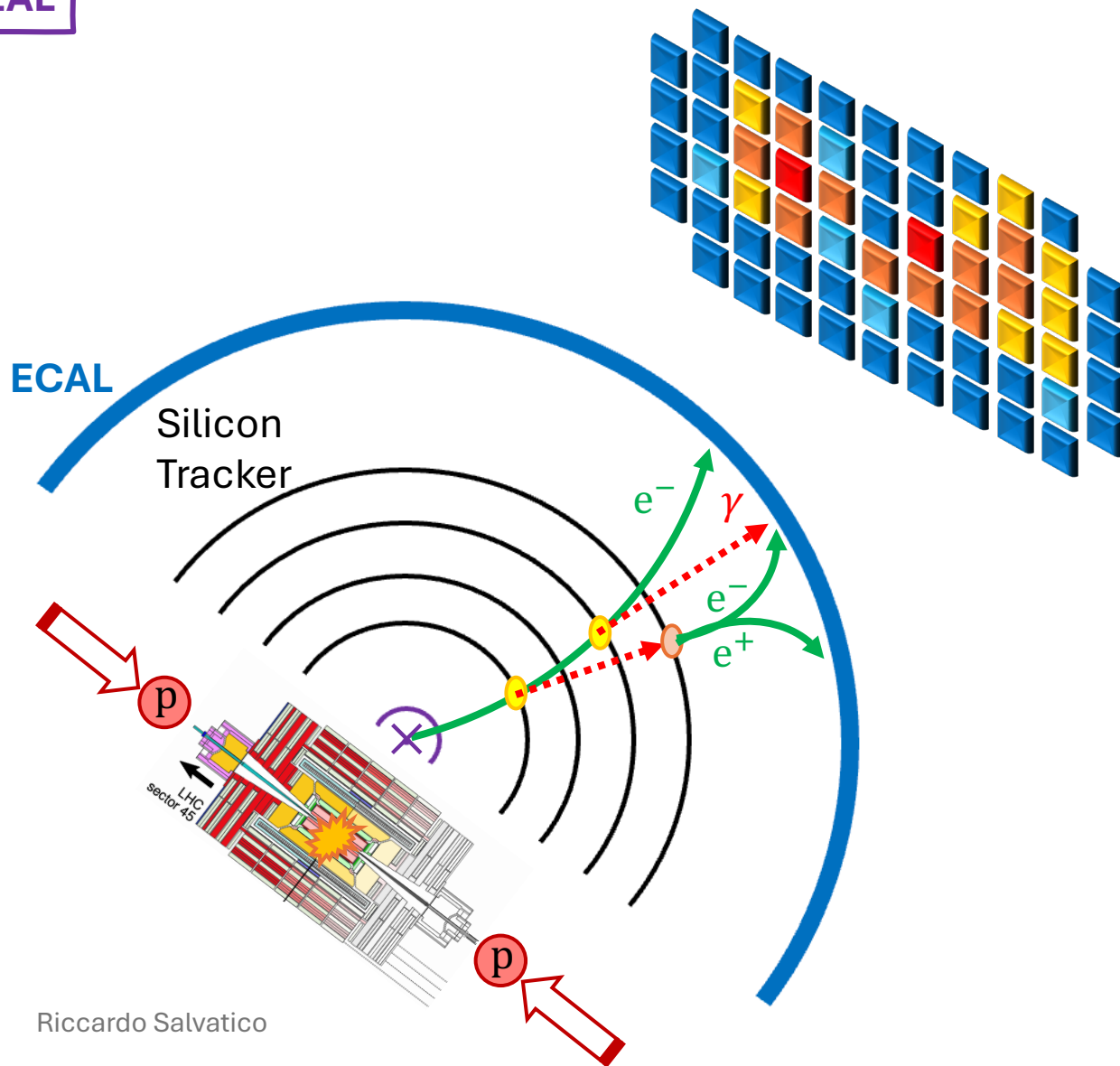
Bremsstrahlung and photon conversions need to be associated to the same initial particle

→ Supercluster



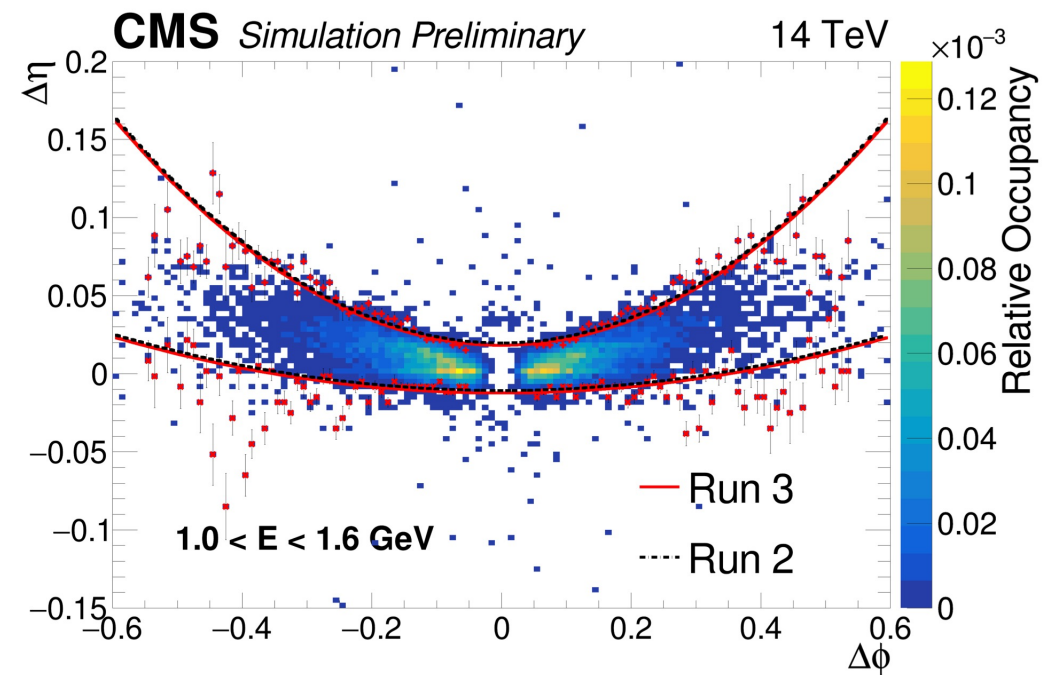


REAL



Bremsstrahlung and photon conversions need to be associated to the same initial particle

→ Supercluster

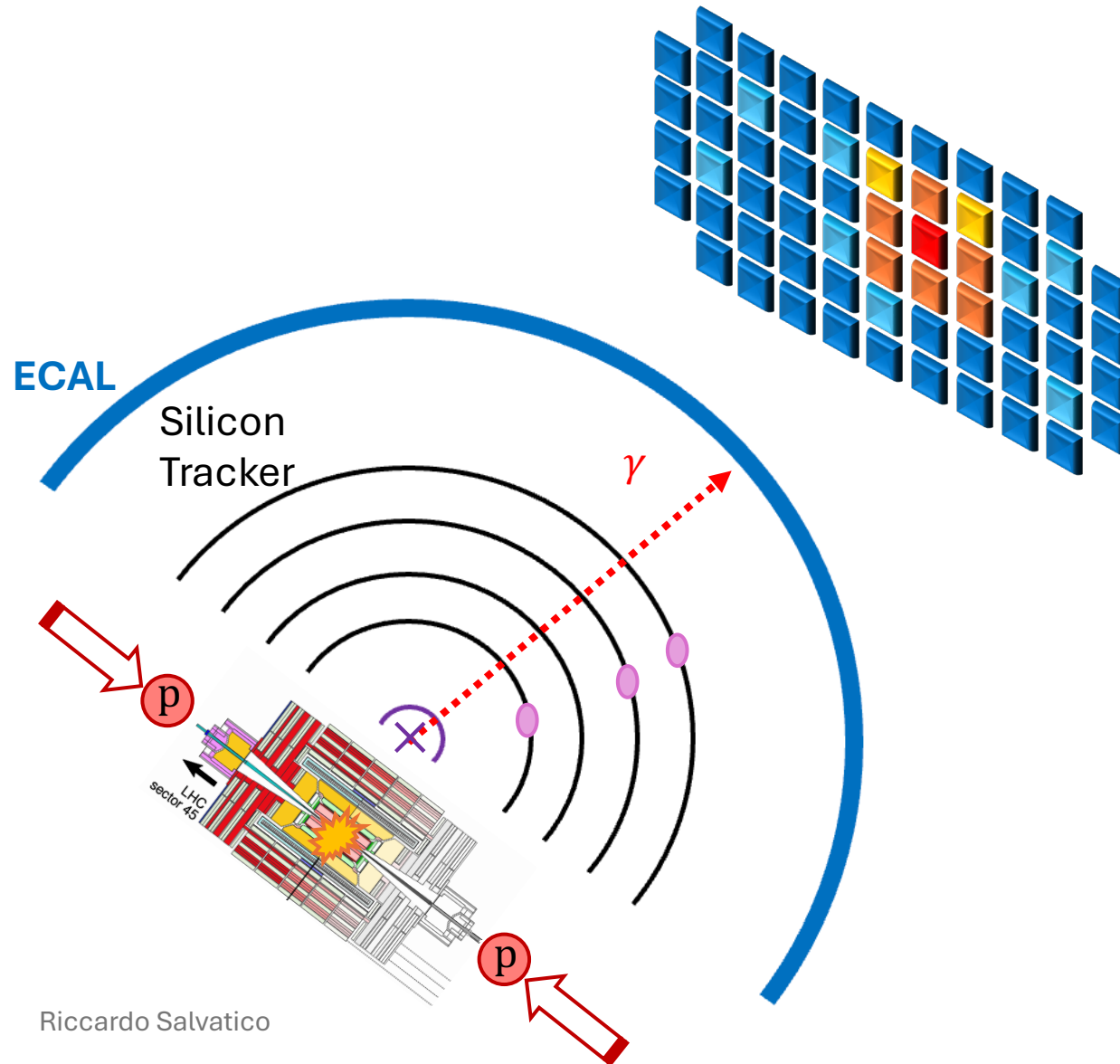


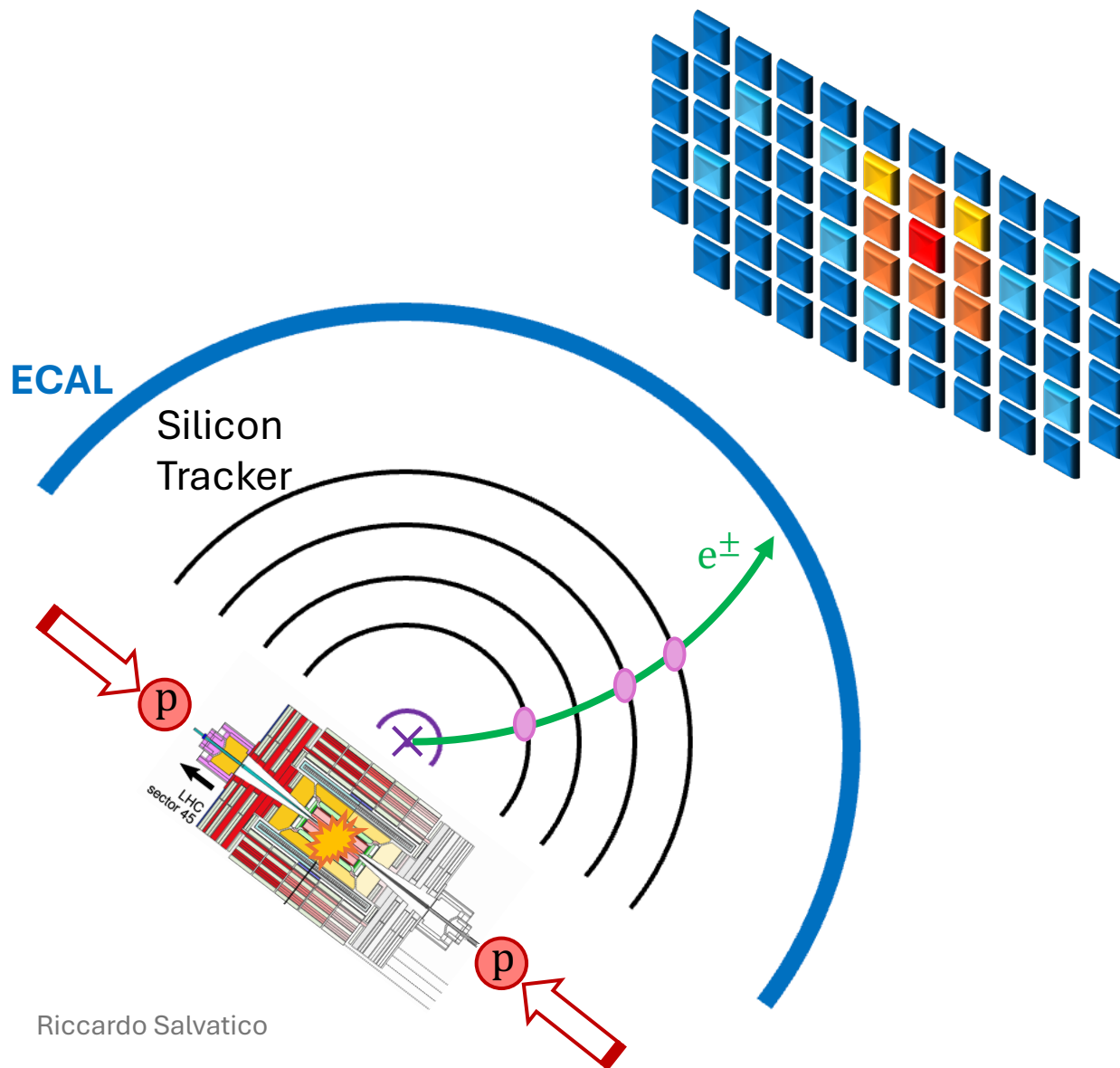
Geometrical procedure that considers the slight bending in  $\eta$  of the low- $p_T$  constituents of EM showers → **moustache**. The moustache was retuned for Run3 to reduce the noise.



Energy deposit in the ECAL

→ photon



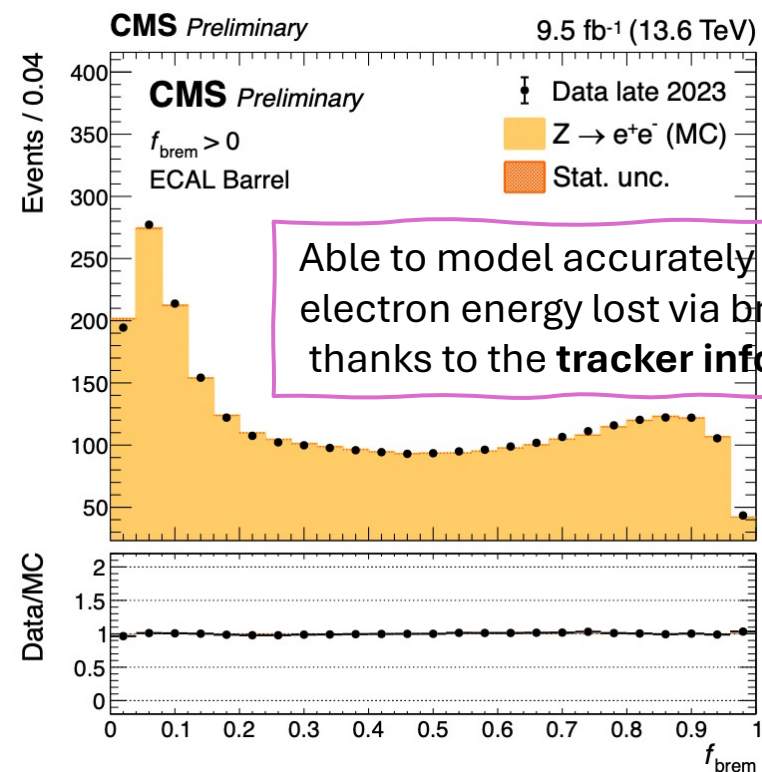


Riccardo Salvatico



Energy deposit in the ECAL + track association


→ **electron/positron**

Using **special track reconstruction algorithm** (Gaussian-sum filter) to consider energy losses via photon radiation. [CMS Note 2005/001](#)



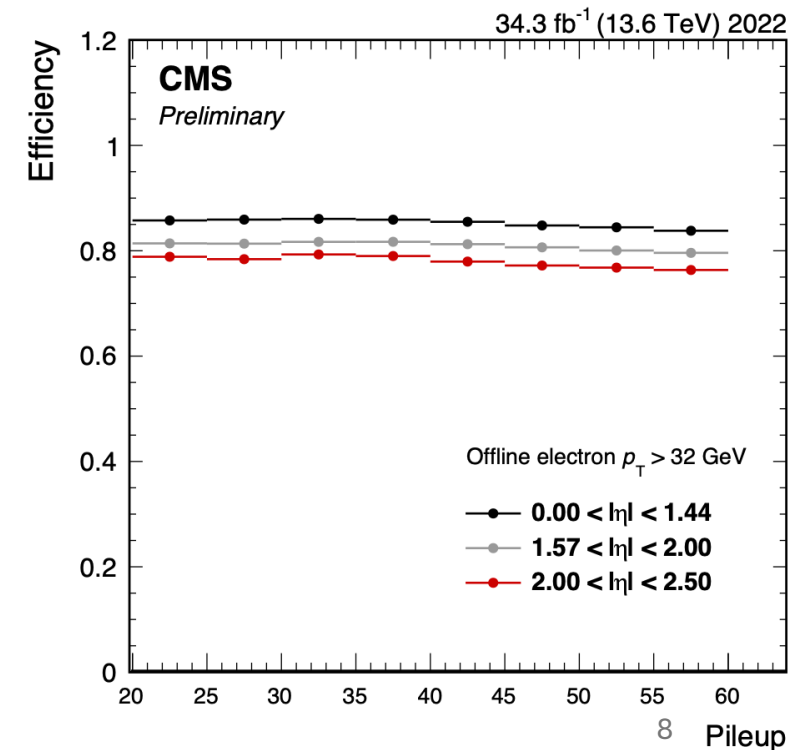
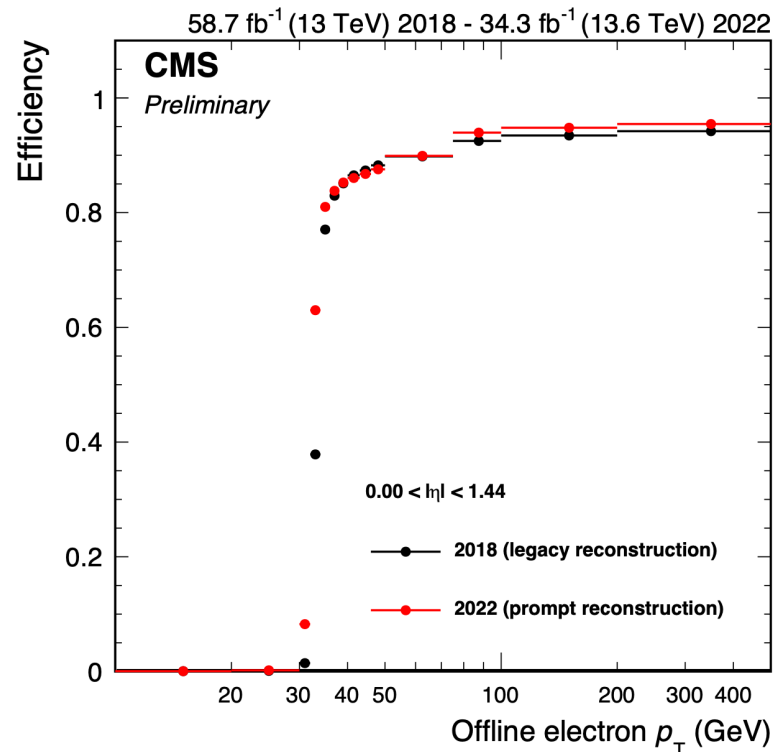
The CMS trigger system selects the collision events to save for further analysis. It is two-tiered:

  **L1**: hardware-based, using on-detector electronics. Saves  $\sim 110$  kHz.

 **HLT**: software. Runs a simpler ( $\rightarrow$  faster) version of the offline reconstruction, allowing us to access data quality and physics content “online”, during collisions. Saves  $\sim 1.5$  kHz.


## High-purity single electron trigger


- Excellent HLT performance in Run3
- Great stability vs pileup





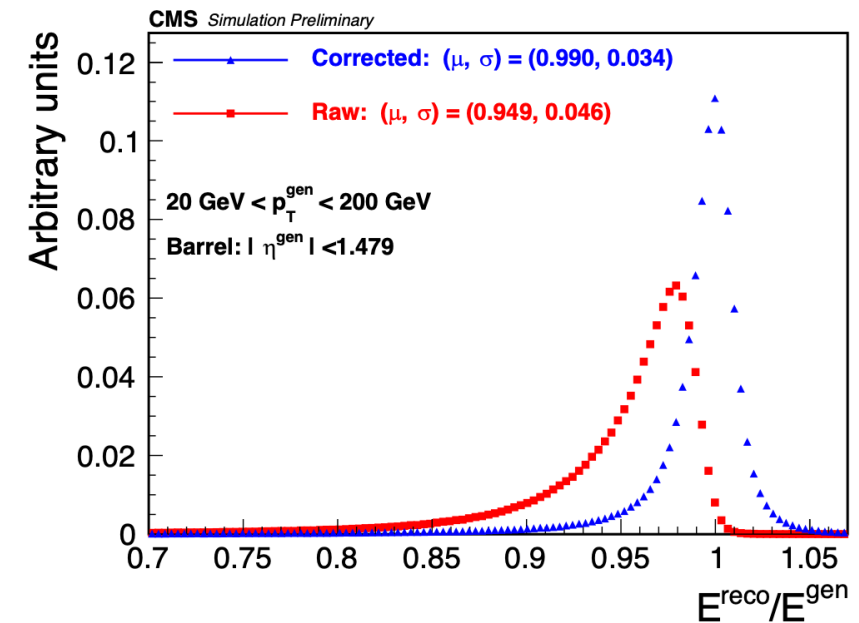
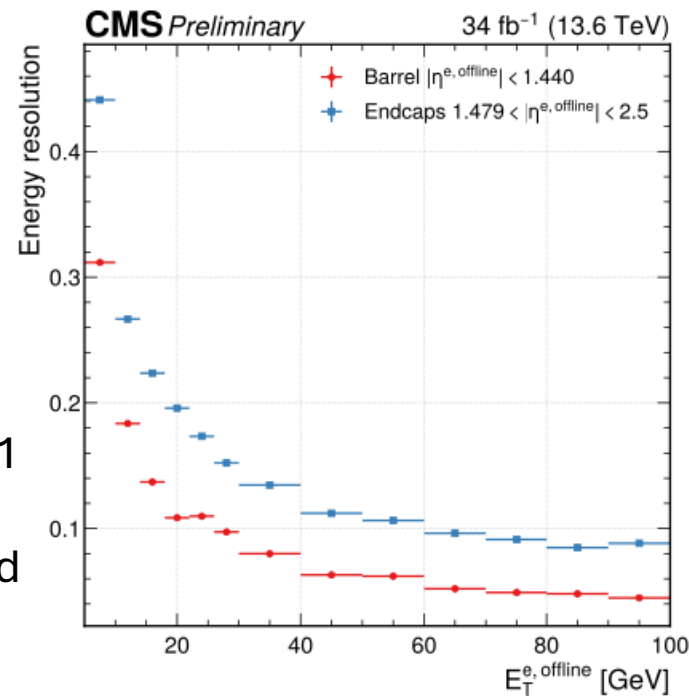
The CMS trigger system selects the collision events to save for further analysis. It is two-tiered:

 **L1**: hardware-based, using on-detector electronics. Saves  $\sim 110$  kHz.

 **HLT**: software. Runs a simpler ( $\rightarrow$  faster) version of the offline reconstruction, allowing us to access data quality and physics content “online”, during collisions. Saves  $\sim 1.5$  kHz.

## High-purity single electron trigger

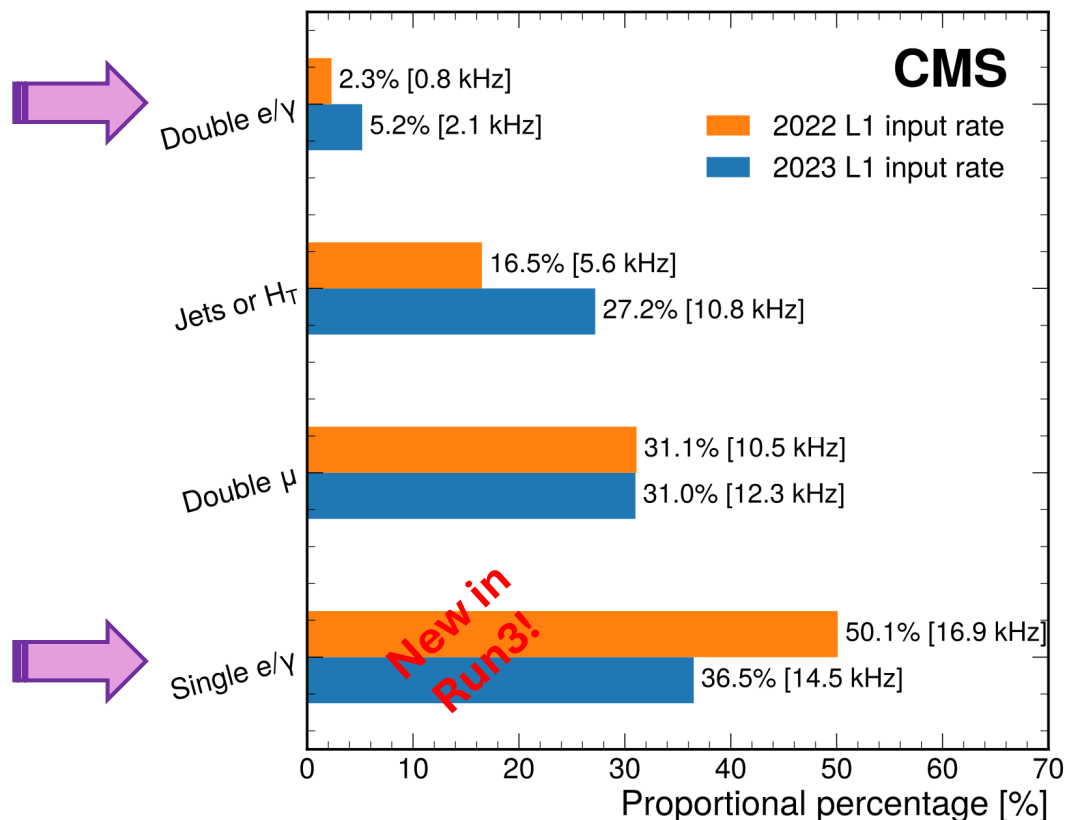
- Excellent HLT performance in Run3
- Great stability vs pileup
- Backed by good  $e/\gamma$  energy resolution at L1
- Supercluster energy response corrected using a BDT-based regression



**HLT scouting:** allow larger rate at low- $p_T$  at the price of giving up the offline reconstruction.

(Can we produce competitive physics results using objects reconstructed online only and with limited event content information?)

[Run2 answer](#))

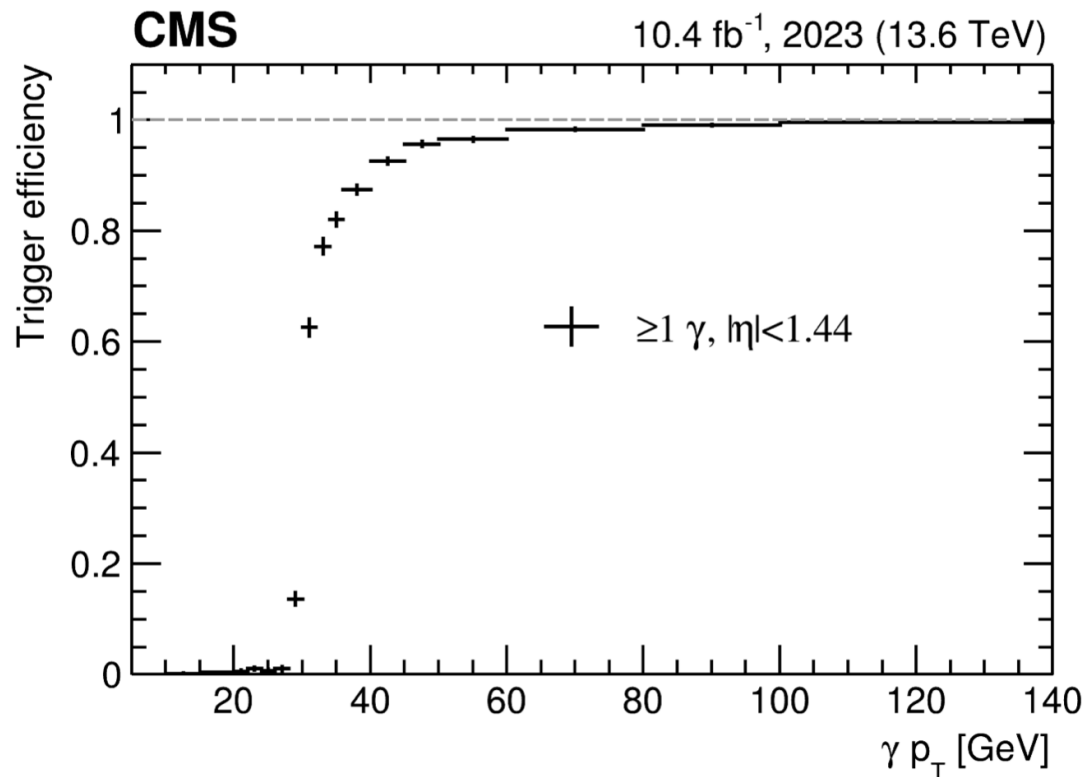


- Large fraction of L1 rate in input to the scouting streams dedicated to single and double  $e/\gamma$ .
- Minimal HLT selection (on supercluster) and thresholds:
  - **30 GeV** for single  $e/\gamma$  → **~ 9.0 kHz HLT** (2023)
  - **12 GeV** for double  $e/\gamma$  → **~ 0.5 kHz HLT** (2023)

**HLT scouting:** allow larger rate at low- $p_T$  at the price of giving up the offline reconstruction.

(Can we produce competitive physics results using objects reconstructed online only and with limited event content information?)

[Run2 answer](#))

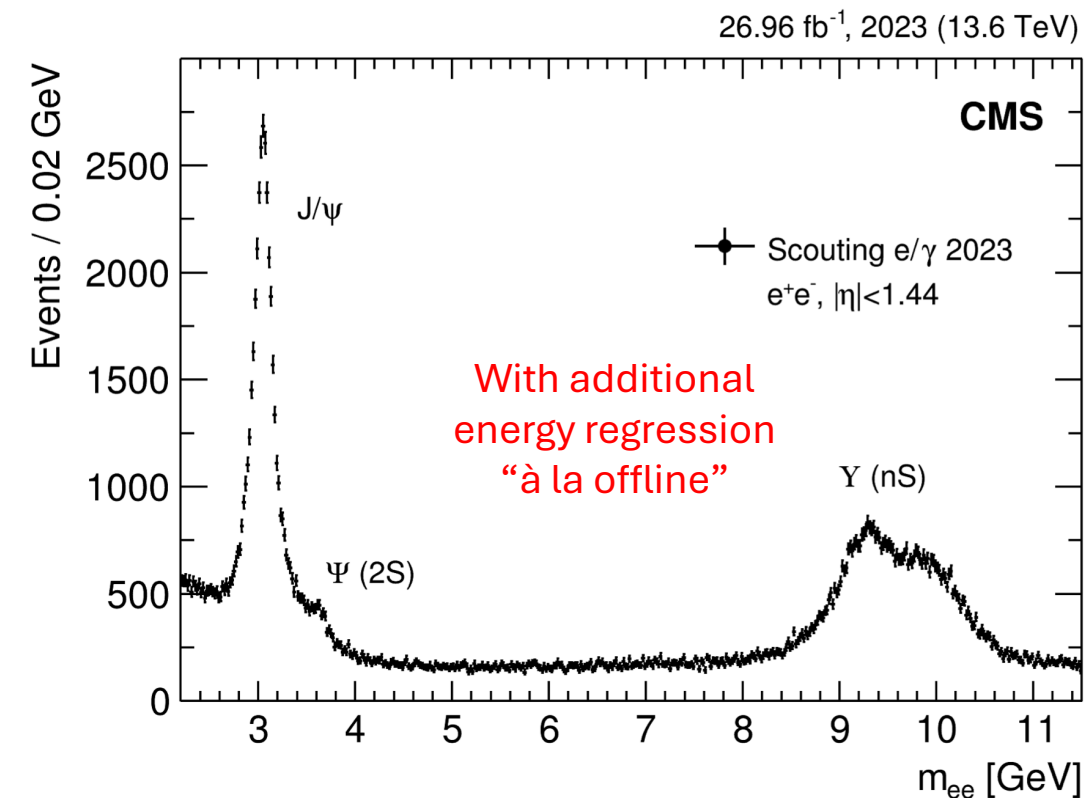


- Large fraction of L1 rate in input to the scouting streams dedicated to single and double  $e/\gamma$ .
- Minimal HLT selection (on supercluster) and thresholds:
  - **30 GeV** for single  $e/\gamma$  → ~ **9.0 kHz HLT** (2023)
  - **12 GeV** for double  $e/\gamma$  → ~ **0.5 kHz HLT** (2023)
- Considerably reduce  $p_T$  thresholds wrt standard HLT, especially for single photon (200 GeV in 2022 and 2023).

**HLT scouting:** allow larger rate at low- $p_T$  at the price of giving up the offline reconstruction.

(Can we produce competitive physics results using objects reconstructed online only and with limited event content information?)

[Run2 answer](#))



- Large fraction of L1 rate in input to the scouting streams dedicated to single and double e/γ.
- Minimal HLT selection (on supercluster) and thresholds:
  - **30 GeV** for single e/γ → ~ **9.0 kHz HLT** (2023)
  - **12 GeV** for double e/γ → ~ **0.5 kHz HLT** (2023)
- Considerably reduce  $p_T$  thresholds wrt standard HLT, especially for single photon (200 GeV in 2022 and 2023).
- Additional low  $p_T$  electrons and photons saved in events recorded using triggers seeded by L1 muons, jets or  $H_T$ .



The **offline reconstruction** is more refined than the online one and allows for further data reprocessing with improved corrections and detector calibration.

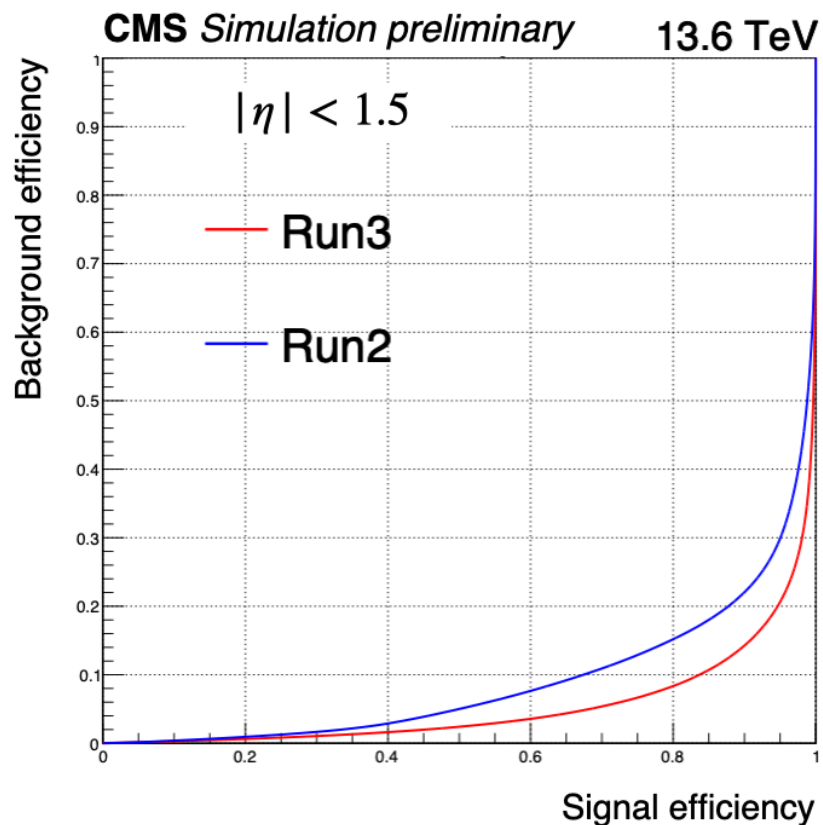
For electrons and photons, this means:

- More “layers” of energy corrections (and potentially more complex models → timing is not a concern)
  - Notably, combination of ECAL energy and tracker momentum measurements to determine the final electron energy, which does not happen at HLT
- More sophisticated IDs
  - Cut-based
    - Flexible – easy to remove unwanted cutoffs at analysis level (e.g., isolation)
  - MVA-based (BDT or DNN)
    - *Generally* stronger signal/background discrimination

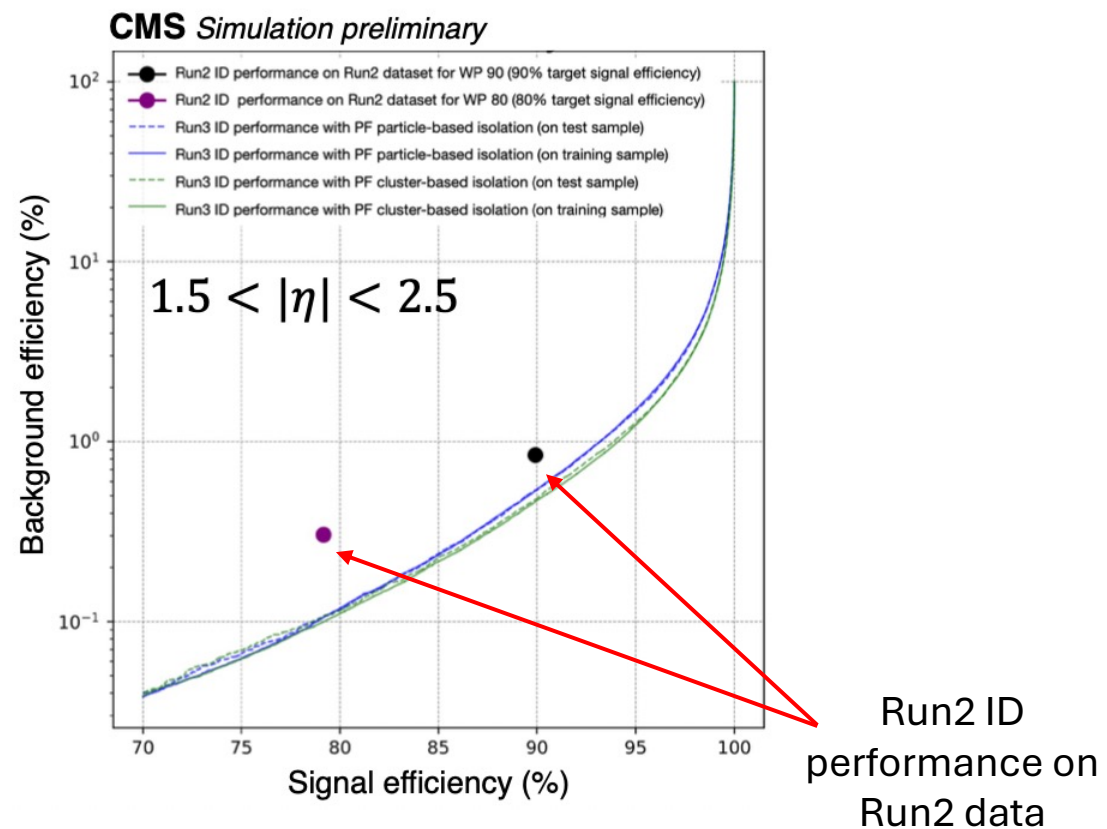


In Run3, the cut-based and MVA-based electron and photon IDs were tuned or retrained to ensure a better performance than the Run2 ones within the Run3 data-taking and detector conditions.

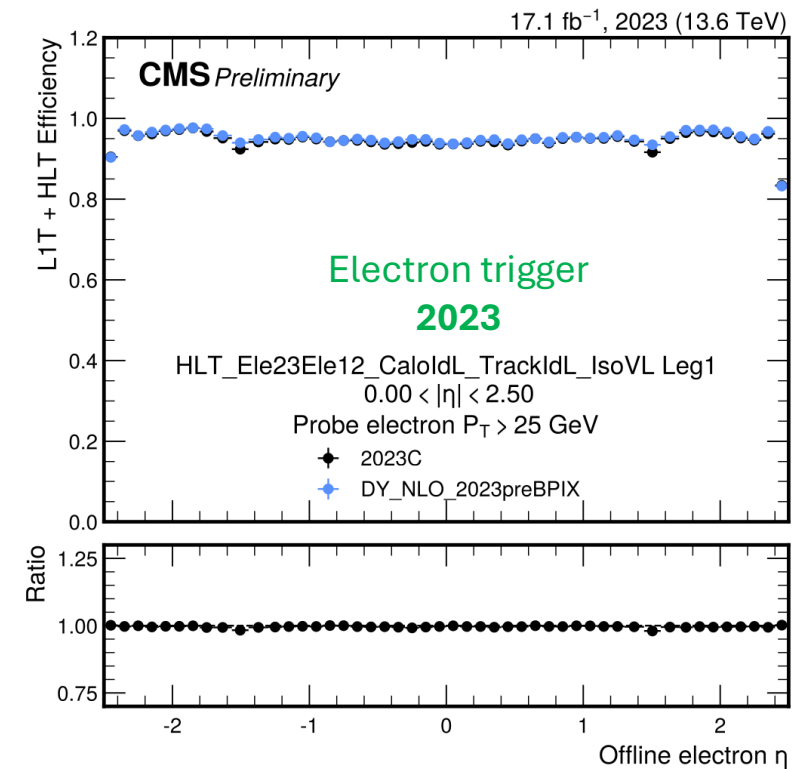
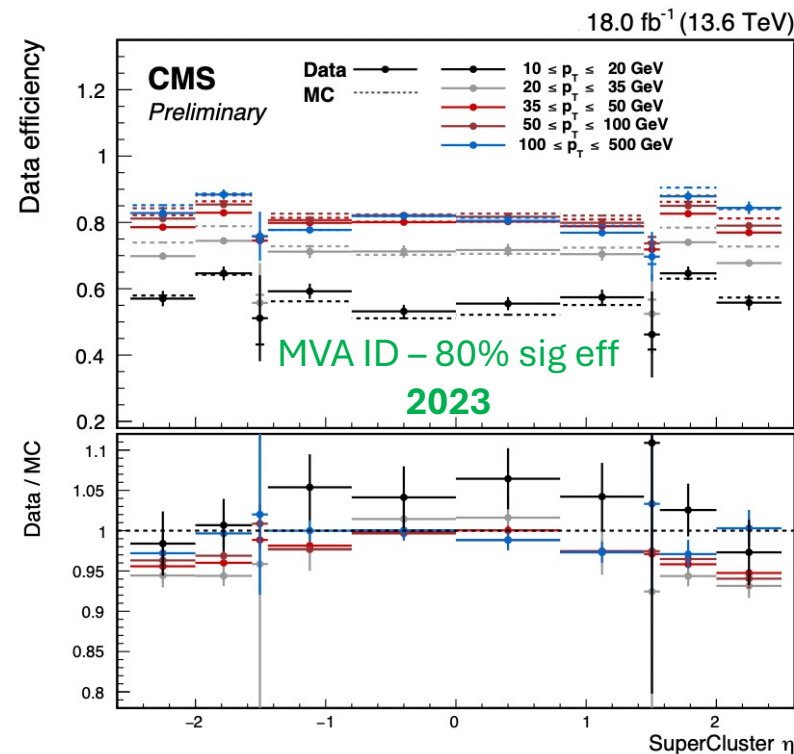
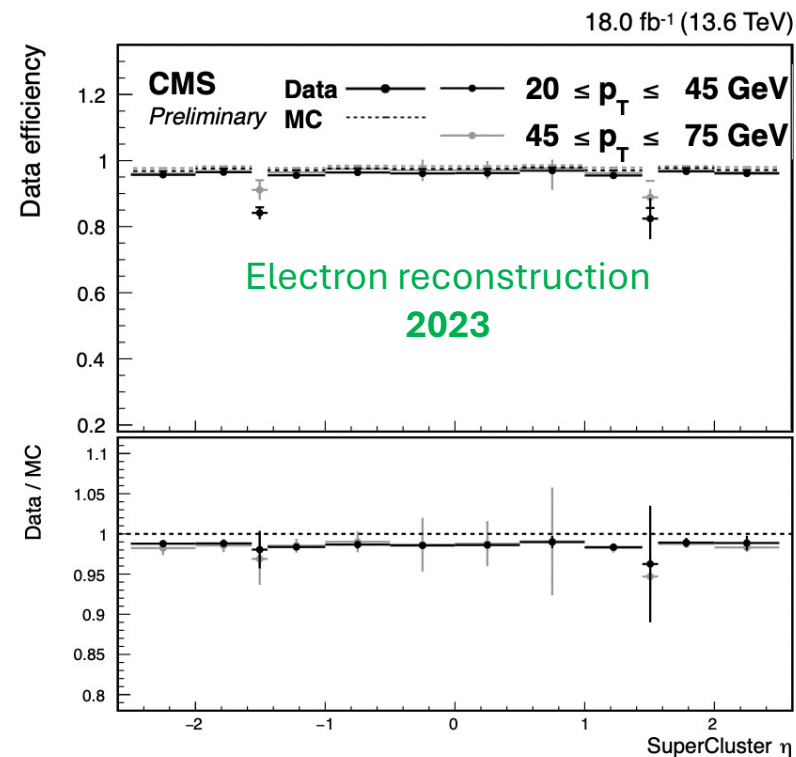
## MVA-based photon IDs



## MVA-based electron IDs



The reconstruction, identification, and trigger performance for electrons and photons is studied in collision data and simulation, and we correct them for discrepancies.



Efficiency to match a supercluster with a track in the tracker

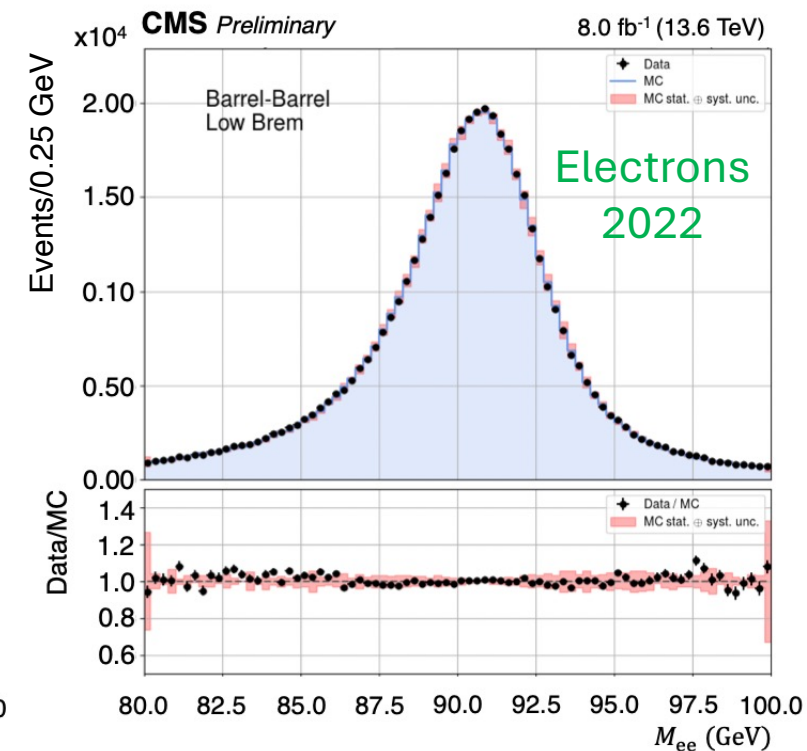
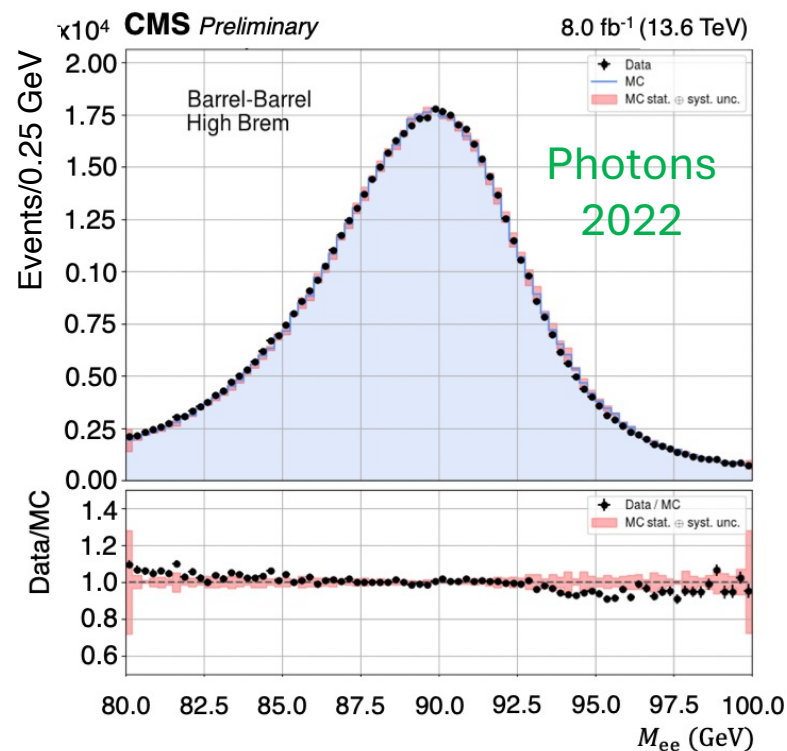
Efficiency to satisfy a set of identification criteria

Efficiency for offline-reconstructed objects to pass a certain trigger

The reconstruction, identification, and trigger performance for electrons and photons is studied in collision data and simulation, and we correct them for discrepancies.

## Scale and resolution corrections

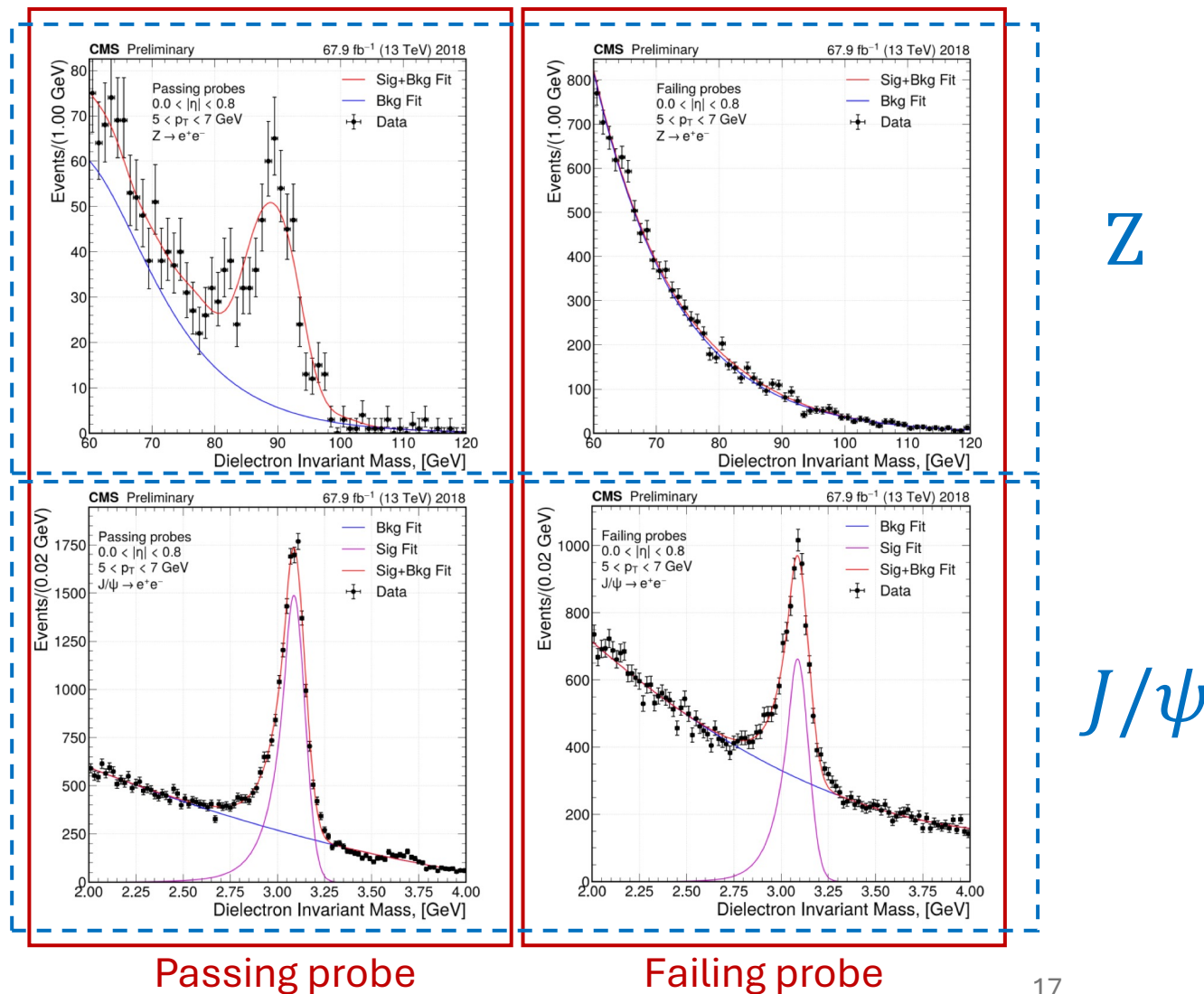
- Derived using electrons from  $Z \rightarrow ee$  for different:
  - particle's  $p_T$  or ECAL amplifier gains
  - detector regions
  - data acquisition runs
  - bremsstrahlung emission
- Scale  $e/\gamma$  energy in collision data
- Spread  $e/\gamma$  energy in simulation



An accurate efficiency measurement for low  $p_T$  ( $< 20$  GeV)  $e/\gamma$  requires a standard candle different from the Z resonance

**$J/\psi$  decays** provide significantly higher statistics and make the measurement possible even below 10 GeV

- *Tag & Probe*: signal peaks clearly visible in both passing and failing probe  $m(ee)$  distributions.



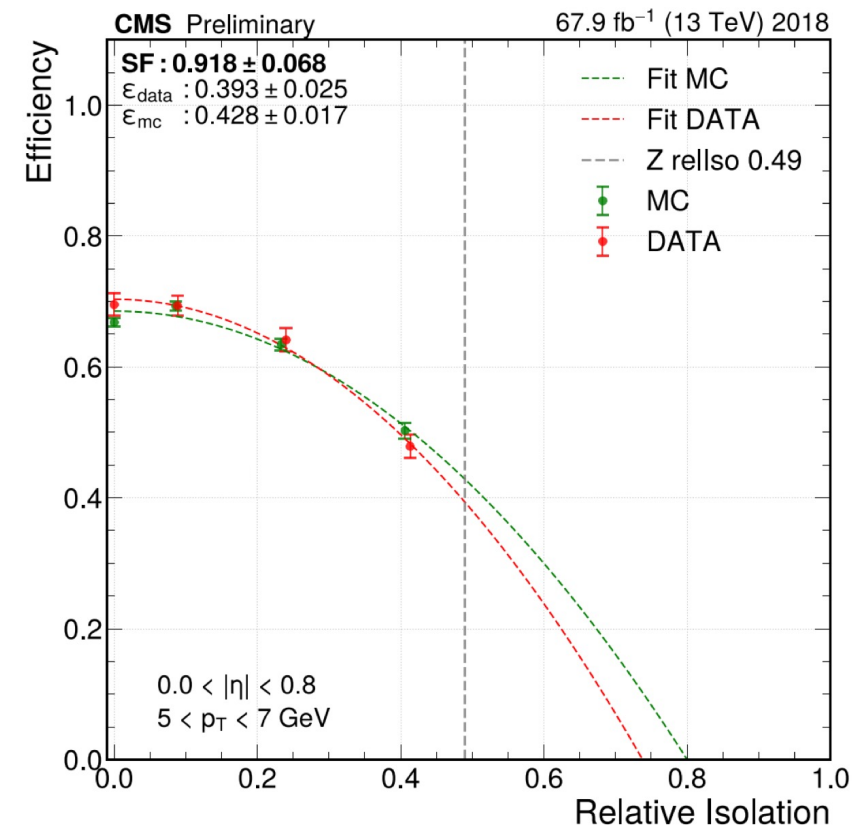
An accurate efficiency measurement for low  $p_T$  ( $< 20$  GeV)  $e/\gamma$  requires a standard candle different from the Z resonance

**$J/\psi$  decays** provide significantly higher statistics and make the measurement possible even below 10 GeV

- *Tag & Probe*: signal peaks clearly visible in both passing and failing probe  $m(ee)$  distributions.

$J/\psi$ s electrons tend to be less isolated than Z electrons

- Extrapolate efficiency at the Z relative isolation value from a fit to the trend of the  $J/\psi \rightarrow ee$  efficiency for different relative isolation bins.







## Supercluster

- Base component in the reconstruction of photons and electrons
- Essential for the ECAL energy response calibration
- One of the inputs to the [Particle Flow](#) global event reconstruction

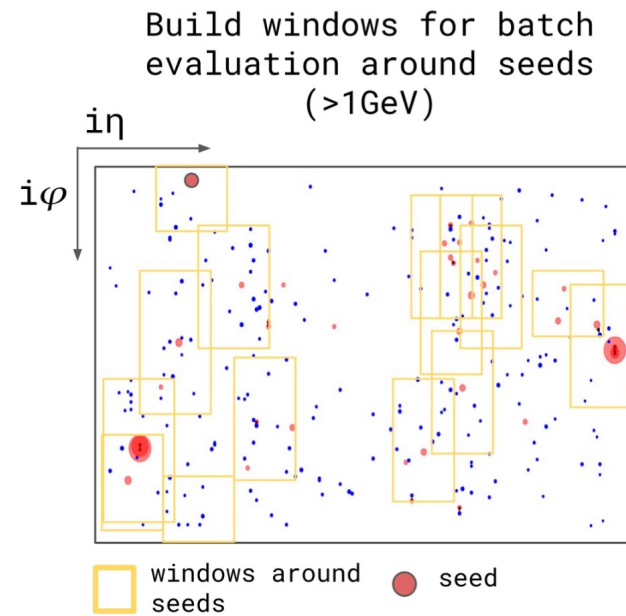
### Moustache

- selects clusters defining a parabolic  $\eta - \phi$  region parametrized by the seed position and the cluster transverse energy
- very efficient but subject to PU/noise contamination – resolution degrades with PU

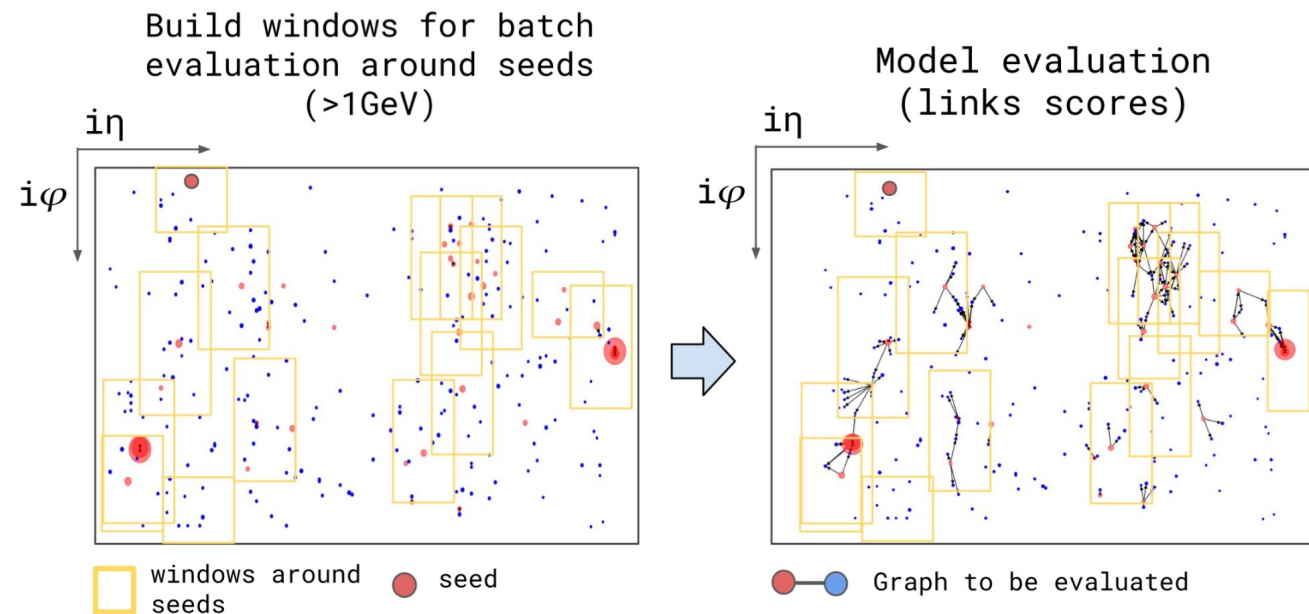
### GNN supercluster → “DeepSC”

- uses small clusters and single crystal hits in a window around the seed
- filters noise/PU *on a cluster-by-cluster basis*, improving the “raw” resolution

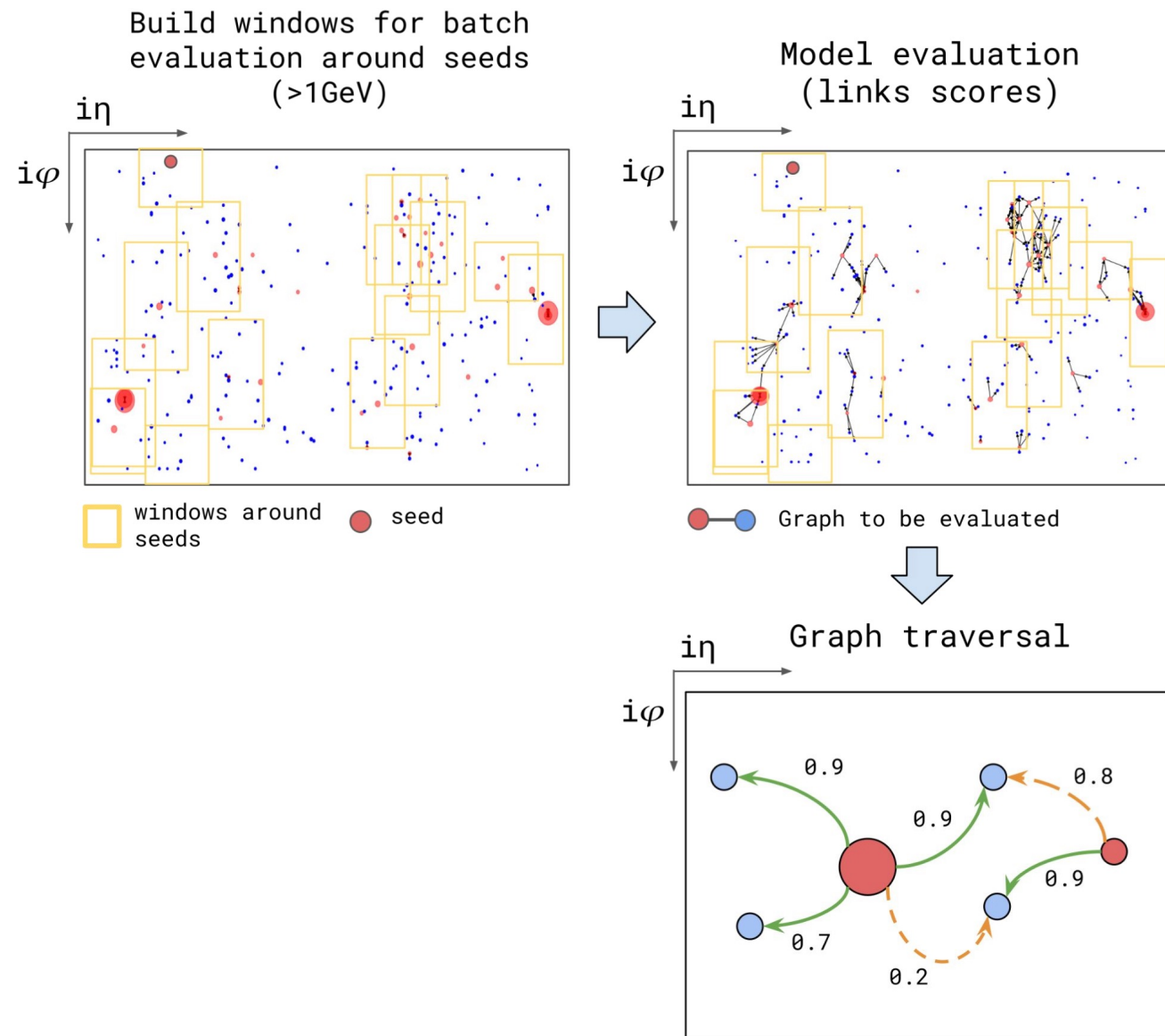
- Build detector windows around each cluster with  $p_T > 1$  GeV (**seed**).



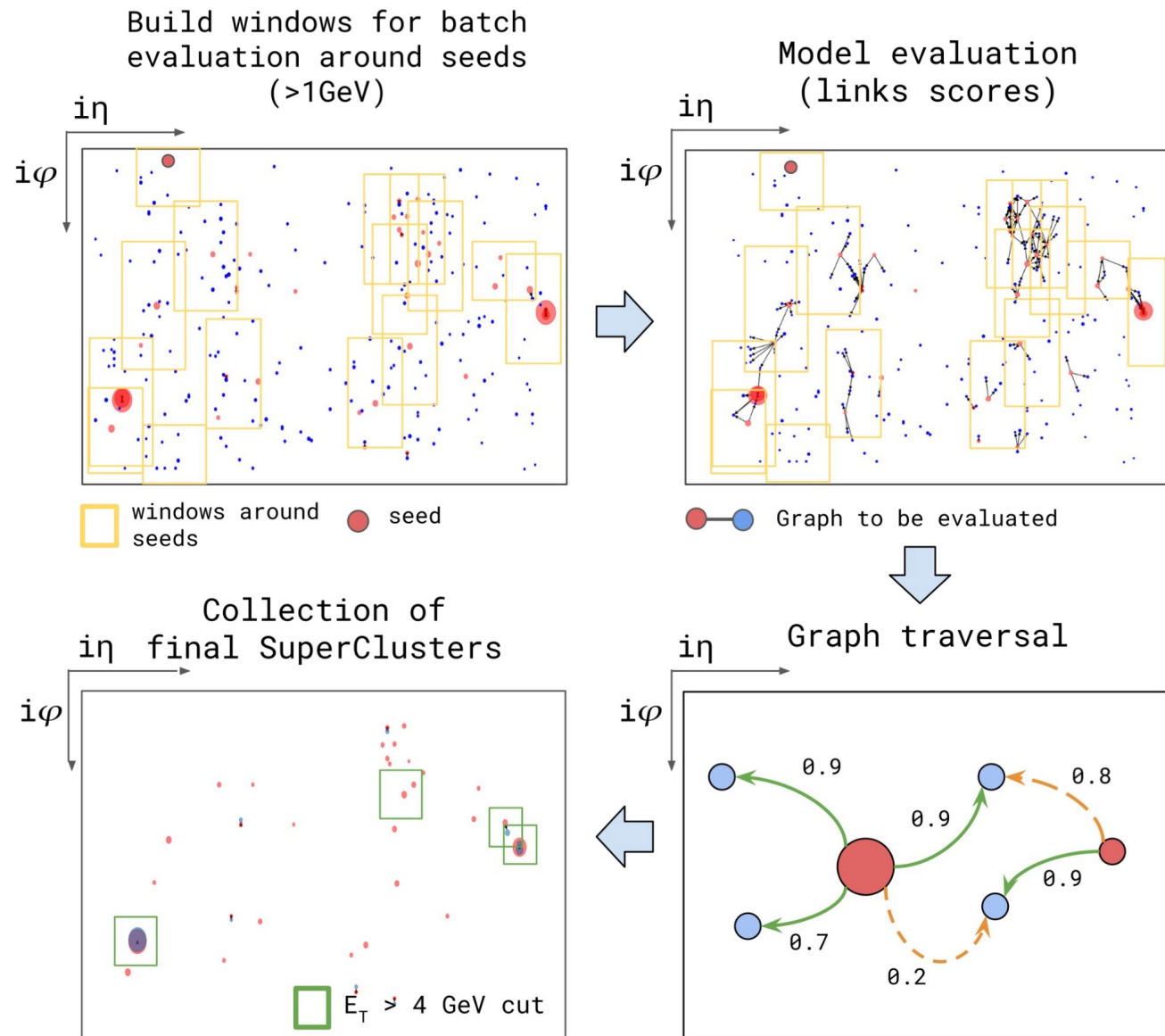
- Build detector windows around each cluster with  $p_T > 1$  GeV (**seed**).
- Connect the seed to all the clusters in each window to form a graph. Use basic cluster properties to evaluate a [TensorFlow](#) model on groups of detector windows: the output is the **probability** of each edge between the seed and the nearby clusters.



- Build detector windows around each cluster with  $p_T > 1$  GeV (**seed**).
- Connect the seed to all the clusters in each window to form a graph. Use basic cluster properties to evaluate a [TensorFlow](#) model on groups of detector windows: the output is the **probability** of each edge between the seed and the nearby clusters.
- Traverse the graph starting from the highest energy seed to choose how to **assign clusters** that can potentially belong to several superclusters.



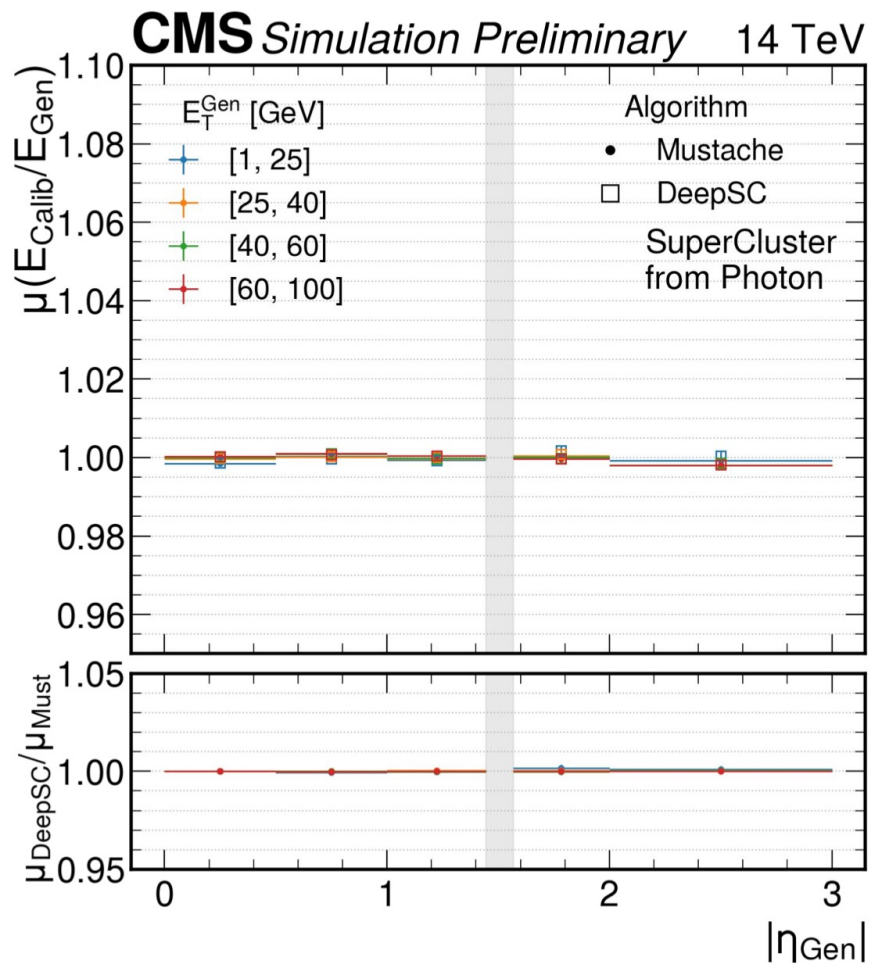
- Build detector windows around each cluster with  $p_T > 1$  GeV (**seed**).
- Connect the seed to all the clusters in each window to form a graph. Use basic cluster properties to evaluate a [TensorFlow](#) model on groups of detector windows: the output is the **probability** of each edge between the seed and the nearby clusters.
- Traverse the graph starting from the highest energy seed to choose how to **assign clusters** that can potentially belong to several superclusters.
- **Apply a cut** of  $p_T > 4$  GeV to remove supercluster formed mainly by detector noise and very low energy pileup.





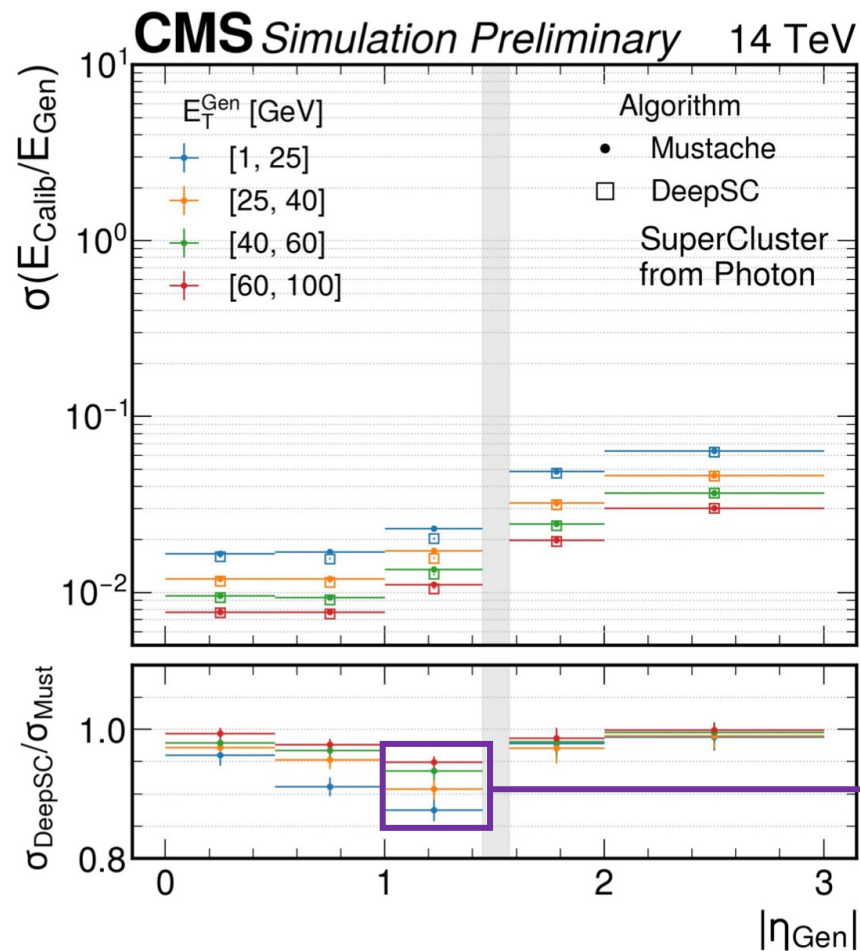
## Energy scale

comparable to the moustache



## Energy resolution

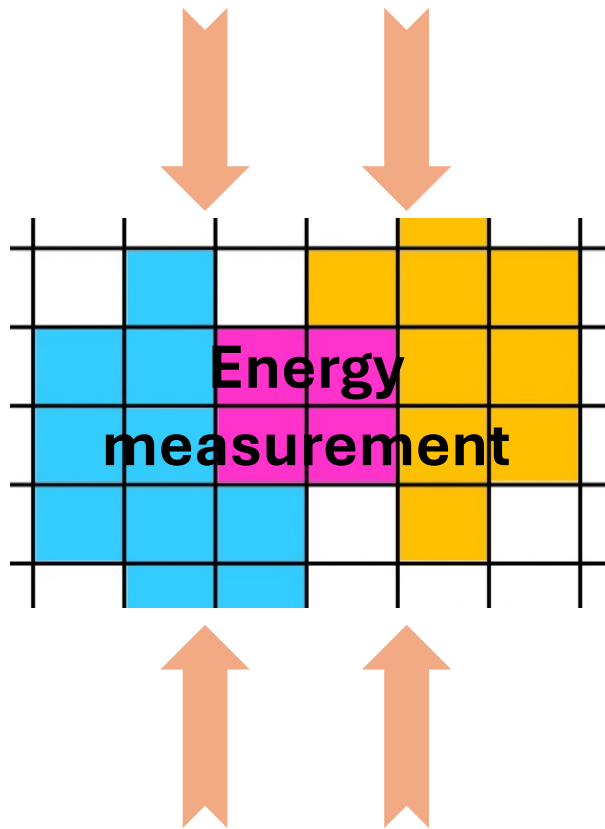
improvements observed across the detector, in particular in the most challenging regions



Region with the largest tracker material budget in front of the ECAL → **largest secondary emissions**



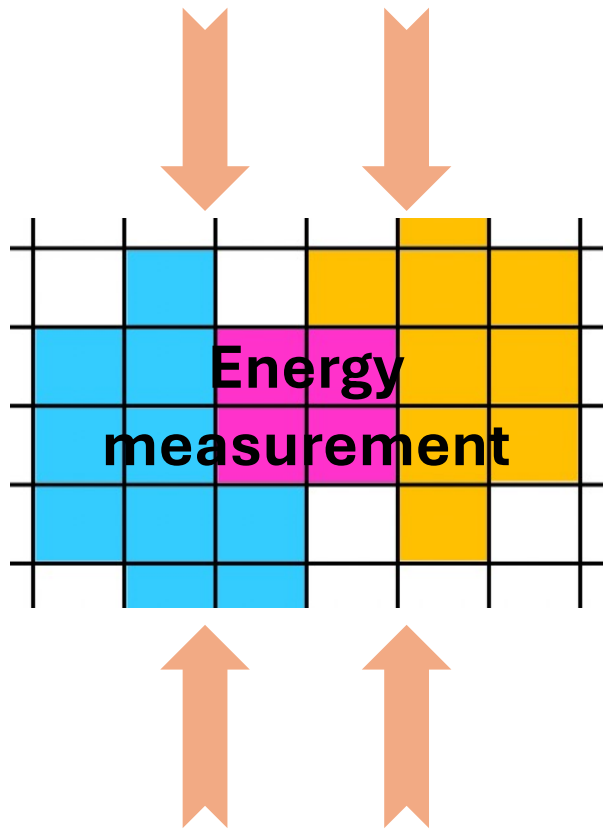
Energy loss in the tracker  
Leakage into the HCAL



Clustering inefficiency  
Finite noise thresholds



Energy loss in the tracker  
Leakage into the HCAL

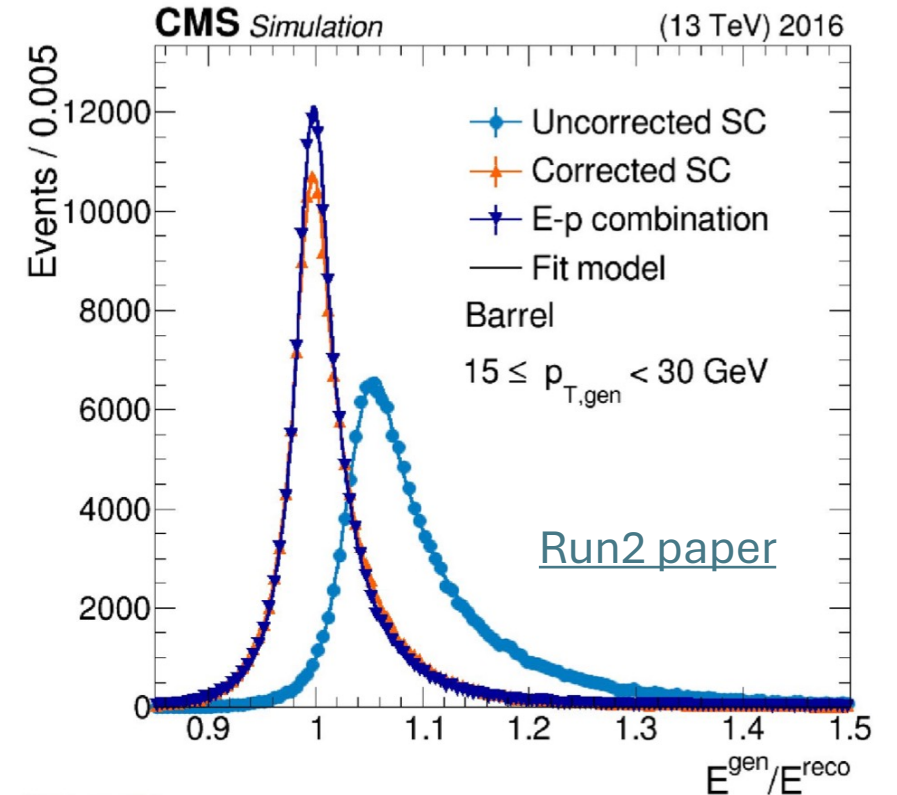


BDT-based **semi-parametric regression**  
using  $\sim 30$  high-level input variables



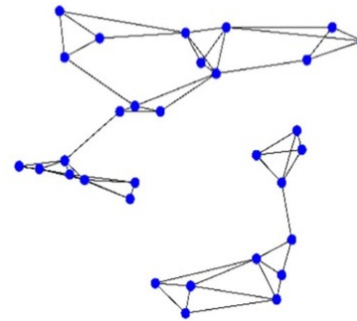
Provide per-object correction  
(supercluster, electron, photon)

Clustering inefficiency  
Finite noise thresholds

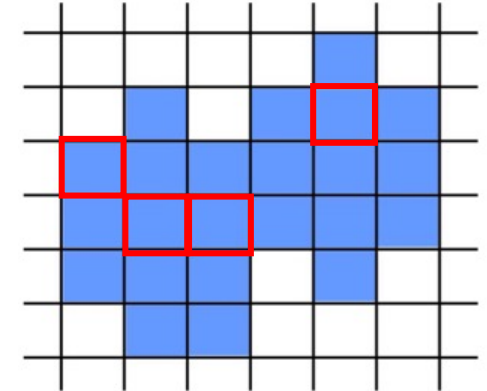


## Dynamic Reduction Network (GNN)

- Allows for variable size input
- Can deal with unordered inputs
- Can handle complicated geometries
- Can handle representation in 4D (x, y, z, energy)

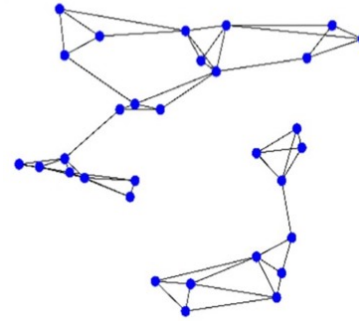
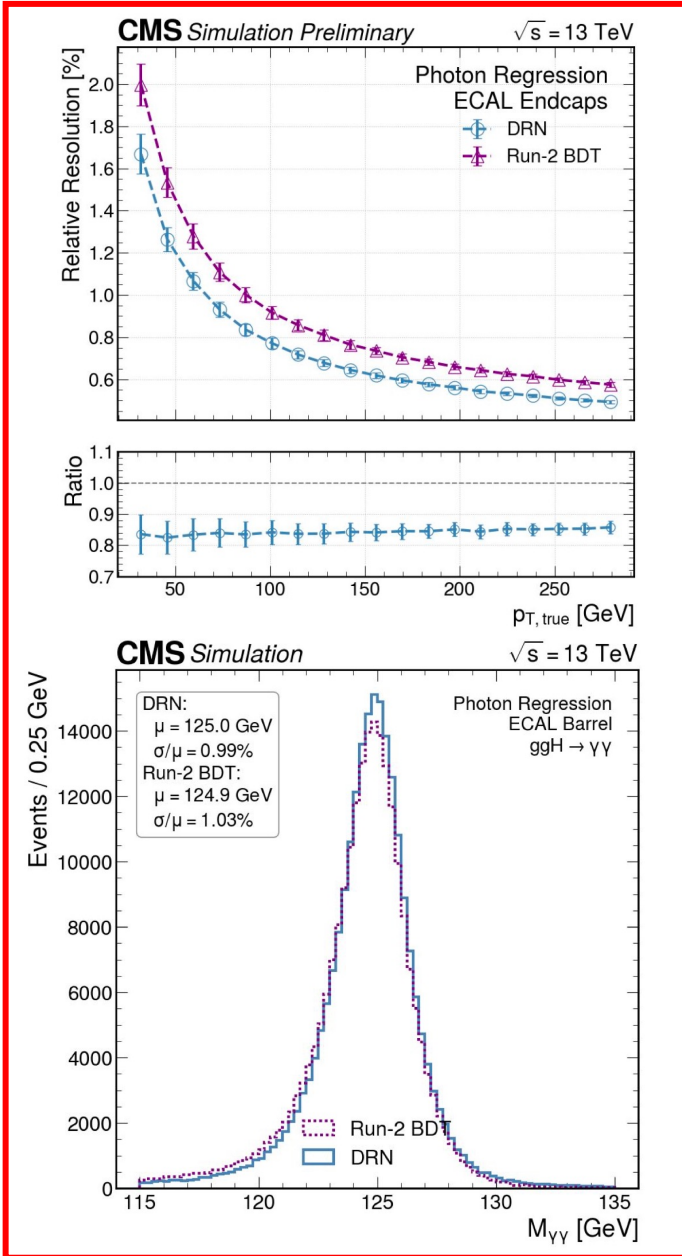


### Single-crystal hits



+

a few higher-level variables  
(median energy density, H/E)



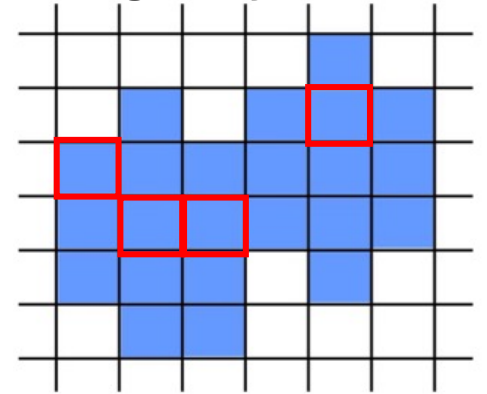
1. Hits are mapped to a multidimensional space

2. GNN learns high-level characteristics from the hits by grouping them based on their similarities

3. The new object is passed through a further NN which maps the learned features to the regression target

~5% improvement in the  $M_{\gamma\gamma}$  resolution in the barrel region!

## Single-crystal hits



+

a few higher-level variables  
(median energy density, H/E)





- Excellent electron and photon reconstruction performance in Run3 – offline and online
  - ✓ Online, the “scouting” trigger extends the reach to lower momentum phase spaces wrt the standard trigger
    - ✓ Can be an asset for several statistically limited searches
  
- Electron and photon IDs were tuned or fully retrained in Run3
  - ✓ Comparable or better identification performance than in Run2
  
- Several types of calibrations and corrections are adopted to ensure the best precision
  - ✓ New methods have been studied that can improve the effectiveness of such corrections, or make the performance measurements more robust or even possible in certain phase spaces (e.g., at low  $p_T$ )
  
- Several ongoing studies using novel techniques are paving the way to more efficient electron and photon reconstruction and more robust energy measurements

**ADDITIONAL MATERIAL**

# The “scale & smearing” corrections

The goal of the scale and smearing corrections is to reduce the residual differences in the electron and photon energy scale and resolution between collision data and simulation. They are derived using electrons from  $Z \rightarrow e^+e^-$  and they:

- scale the electron energy in data:  $M_{ee}^{\text{scaled}} = M_{ee} \sqrt{(1 + \Delta P_{e1})(1 + \Delta P_{e2})}$ , where  $\Delta P_{ei}$  is the scale shift with respect to MC for electron “i”;
- smear the electron energy in the simulation:  $M_{ee}^{\text{smearred}} = M_{ee} \sqrt{\text{Gaus}(1, \Delta C_{e1}) \text{Gaus}(1, \Delta C_{e2})}$ , where  $\Delta C_{ei}$  is the additional smearing for electron “i”.

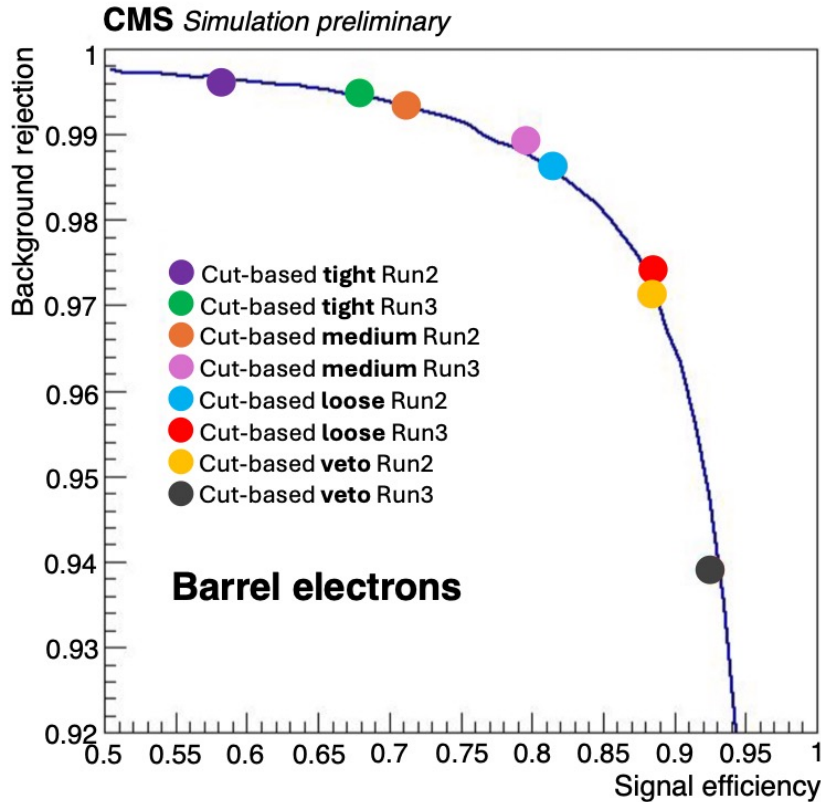
The variables  $\Delta P_{ei}$  and  $\Delta C_{ei}$  are determined by minimizing a global binned negative log-likelihood of the invariant mass for each di-electron category. The categories are defined by subdividing events according to the data acquisition run number, the ECAL amplifier gain, and the electron  $\eta$ ,  $p_T$ , and  $R_9$ .

The derivation of scale and smearing corrections for photons uses electrons from Z boson decay reconstructed as photons by the CMS software, and to which the photon energy regression was applied.

# Choice of new regression architecture

Can it (easily) handle...	BDT	MLP	CNN	RNN	GNN
Variable-size input	X	X	✓	✓	✓
Complicated geometries	✓	✓	X	✓	✓
4D inputs	✓	✓	X	✓	✓
Unordered inputs	X	X	✓	X	✓

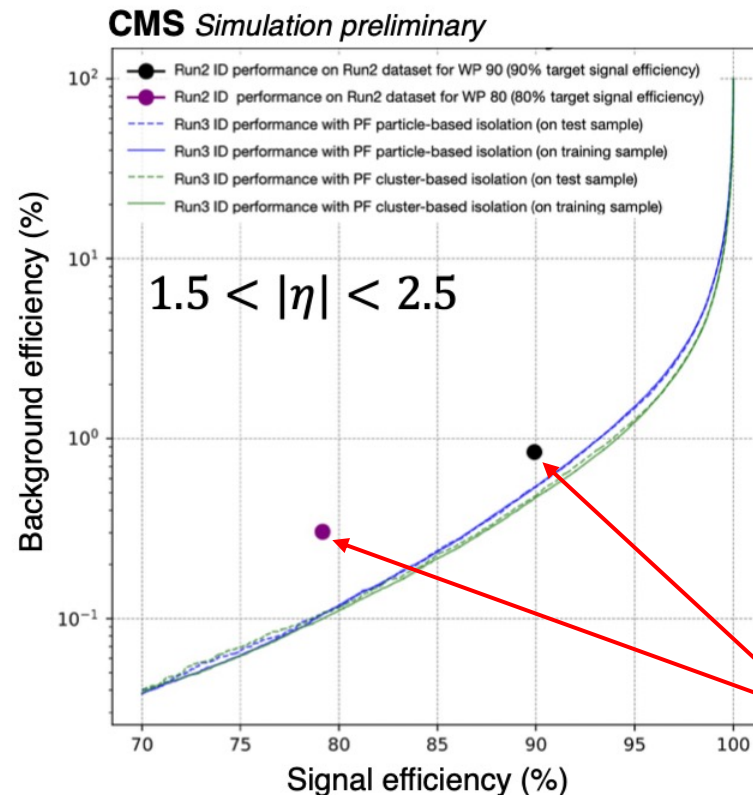
In Run3, the cut-based and MVA-based electron and photon IDs were tuned or retrained to ensure a better performance than the Run2 ones within the Run3 data-taking and detector conditions.



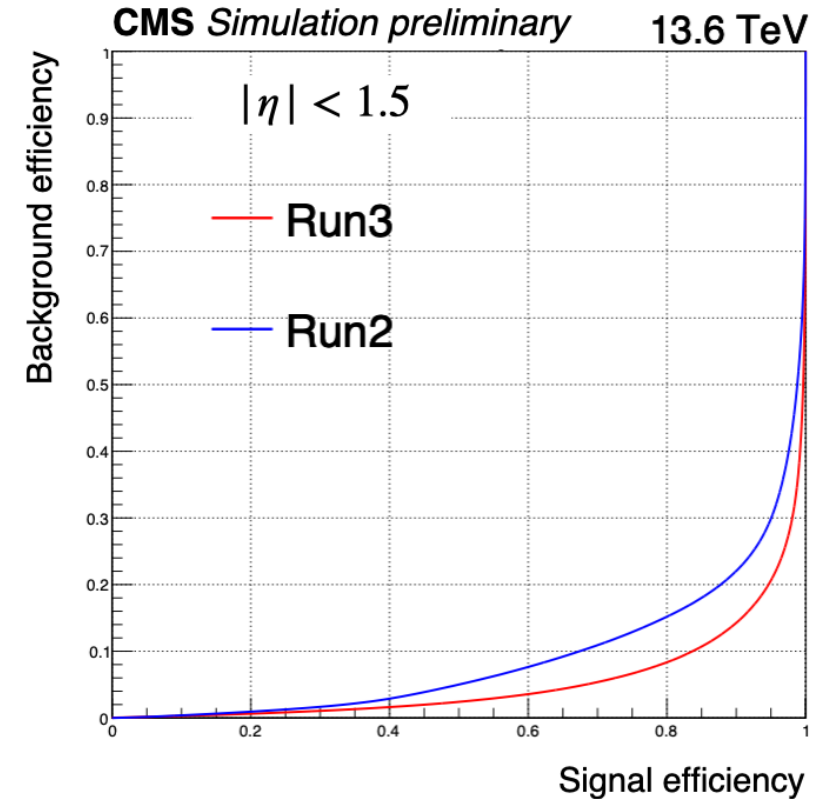
## Cut-based electron IDs

Riccardo Salvatico

## MVA-based electron IDs



Run2 ID  
performance on  
Run2 data



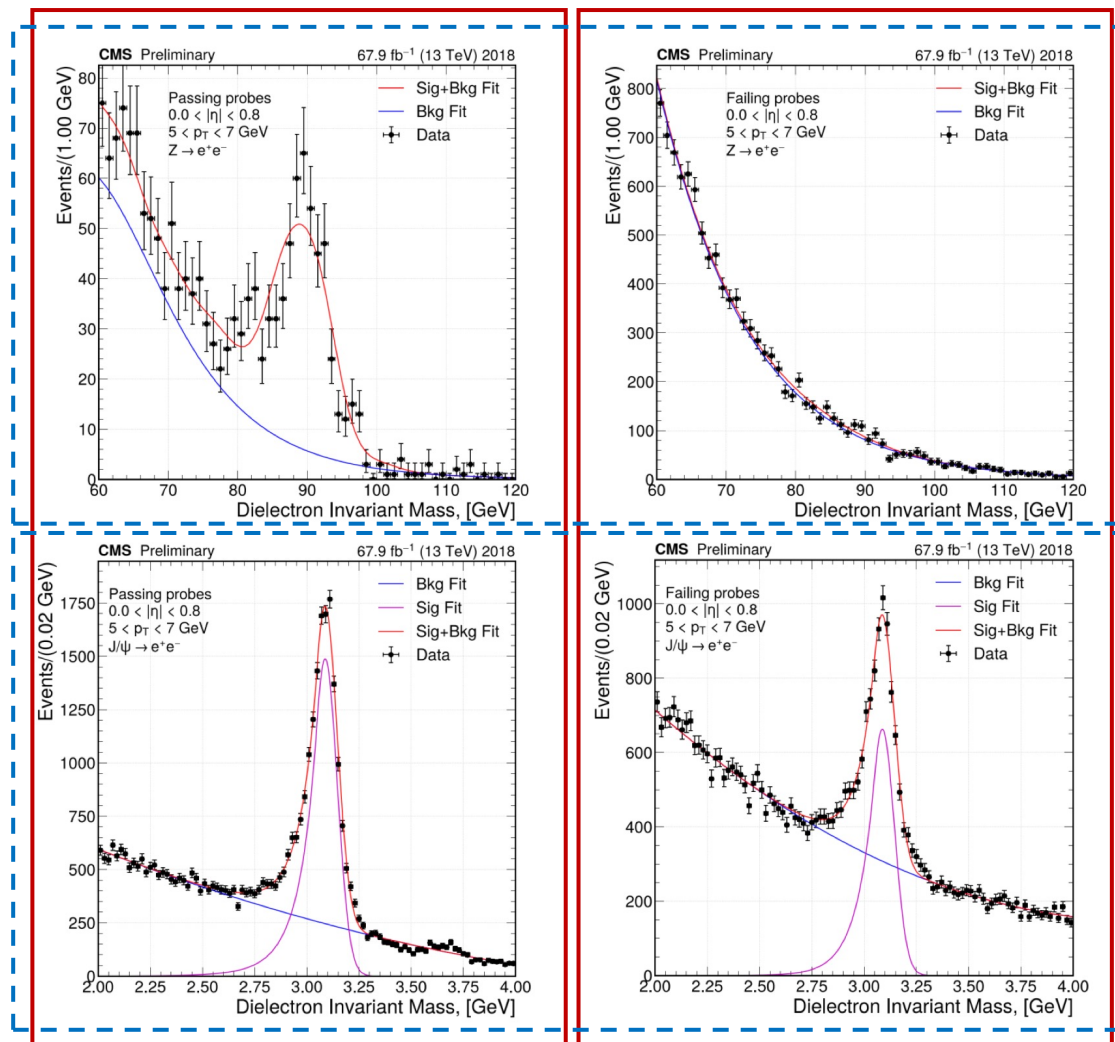
## MVA-based photon IDs

An accurate efficiency measurement for low  $p_T$  ( $< 20$  GeV)  $e/\gamma$  requires a standard candle different from the Z resonance



**$J/\psi$  decays** provide significantly higher statistics and make the measurement possible even below 10 GeV

- Tag & Probe: signal peaks clearly visible in both passing and failing probe  $m(ee)$  distributions.



Z

$J/\psi$

Passing probe

Failing probe

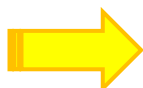


An accurate efficiency measurement for low  $p_T$  ( $< 20$  GeV)  $e/\gamma$  requires a standard candle different from the Z resonance



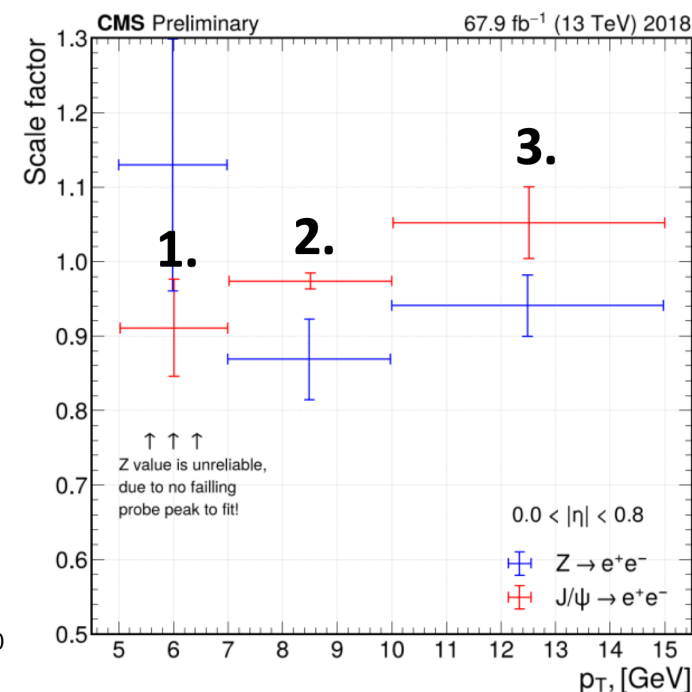
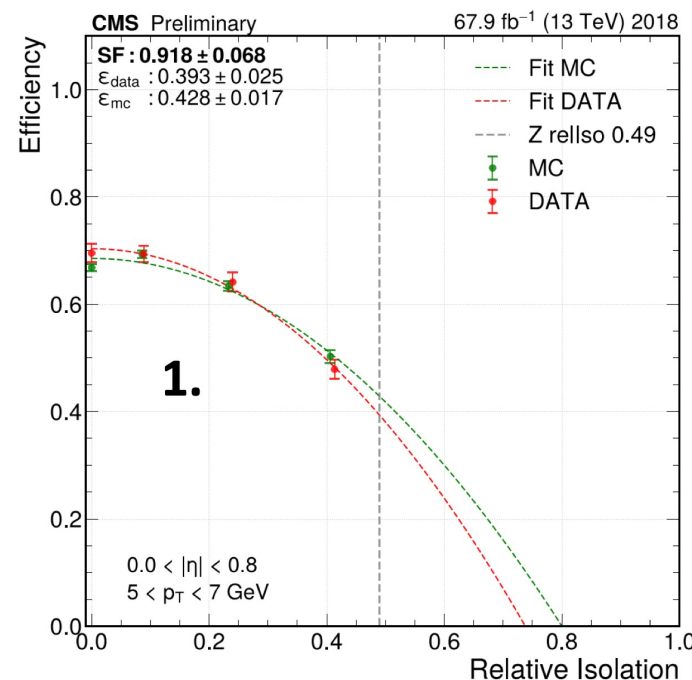
$J/\psi$  decays provide significantly higher statistics and make the measurement possible even below 10 GeV

- Tag & Probe: signal peaks clearly visible in both passing and failing probe  $m(ee)$  distributions.



$J/\psi$ s electrons tend to be less isolated than Z electrons

- Studied a method to make reliable measurements of ID efficiencies when the IDs contain isolation requirements



- I. Measure the electron ID efficiencies from  $J/\psi$  events in different ( $p_T, \eta$ , **relative isolation**) bins.
- II. Fit the trend of efficiency measured in step I. vs relative isolation for each ( $p_T, \eta$ ) bin.
- III. Take the efficiency value obtained by interpolating the measurements done in step I. with the fit done in step II. at the average Z MC relative isolation value in that particular ( $p_T, \eta$ ) bin.